The Abdus Salam International Centre for Theoretical Physics

United Nations Educational, Scientific and Cultural Organization

IAEA International Atomic Energy Agency

2332-29

School on Synchrotron and FEL Based Methods and their Multi-Disciplinary Applications

19 - 30 March 2012

Transmission X-ray Microscopy contrast approaches and applications in life science

Alessandra Gianoncelli

ELETTRA - Sincrotrone Trieste

Strada Costiera 11, 34151 Trieste, Italy - Tel.+39 040 2240 111; Fax +39 040 224 163 - sci_info@ictp.it

Transmission X-ray Microscopy contrast approaches and applications in life science

Alessandra Gianoncelli

ELETTRA – Sincrotrone Trieste

alessandra.gianoncelli@elettra.trieste.it

Different X-ray microscopy techniques:

- **Most of XRMs have an optical analogon to other wavelengths techniques (visible light microscopy, electron microscopy). This means that optical rules can in many cases be applied and transferred from one technique to another.**
- **Same is valid for applying absorption and phase-related imaging contrasts.**

We will try to explore now different transmission XRM techniques...

The classic and most common: X-ray projection imaging

Old Crooke’s apparatus

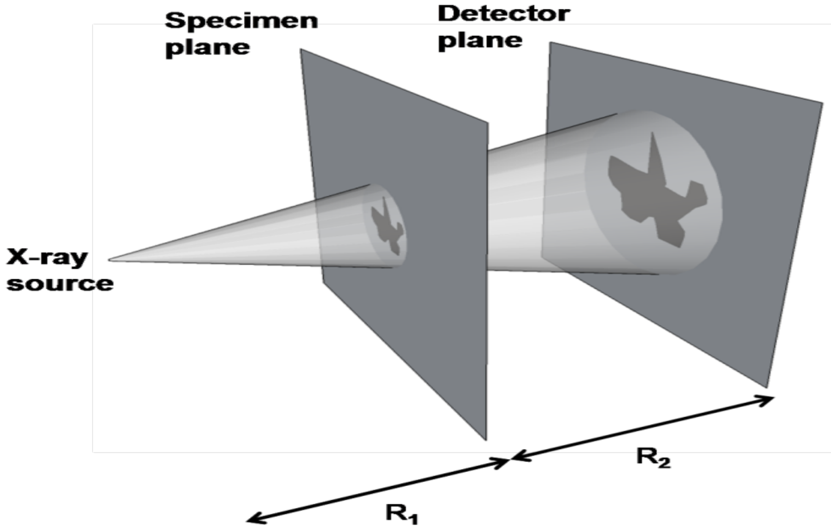

Modern digital radiograph

The magnification M is given by $M=1+R2/R1$, the optical resolution is determined by source size

Problem: Fresnel diffraction
(unsharpening of the image)

Background info: X-ray microscopy types

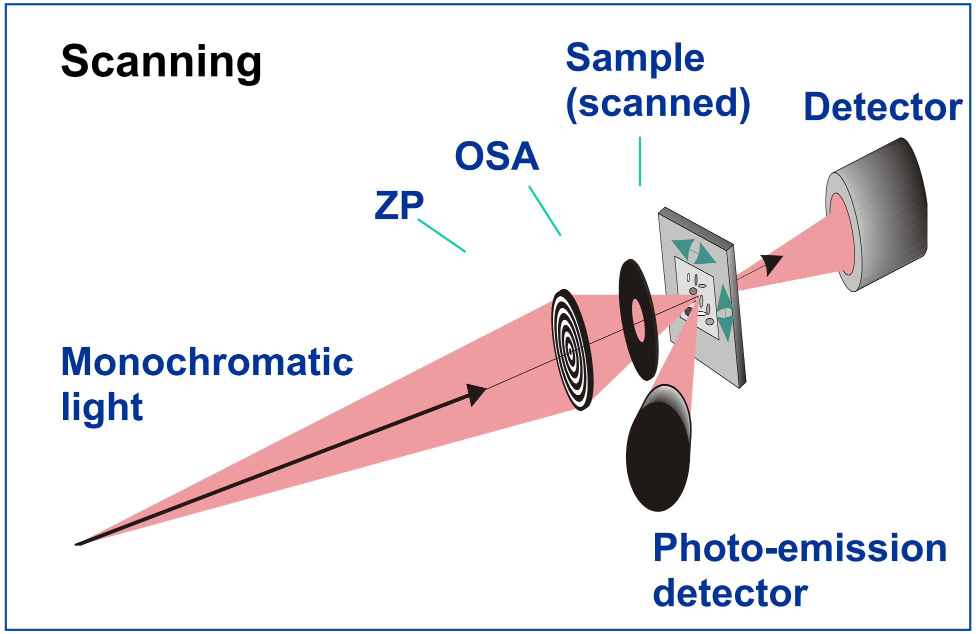

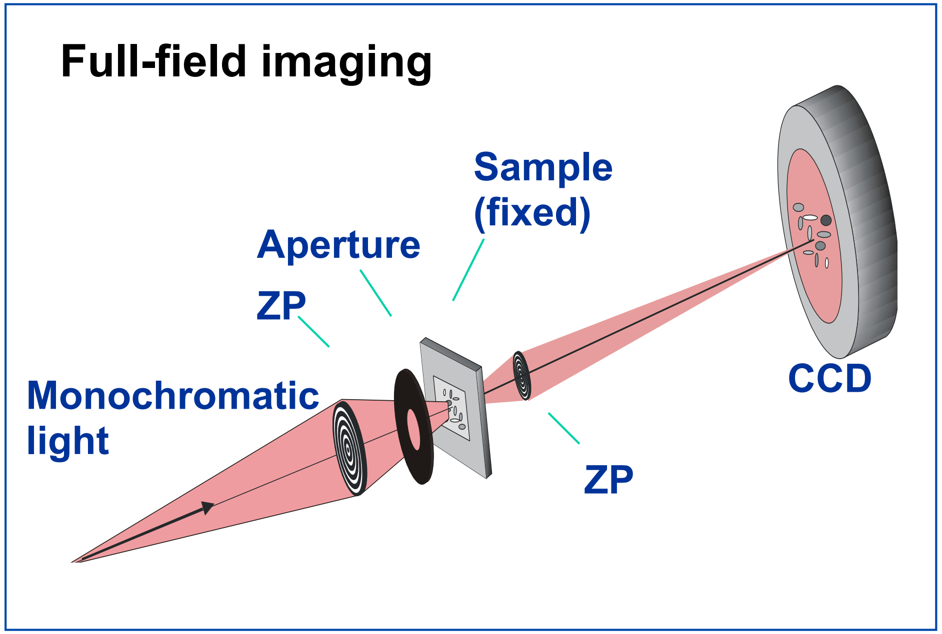

+ versatile detectors can run simultaneously;
+ easier optics set-up;
- long exposure time;
- complex electronics.

Ideal for spectromicroscopy

+ short exposure time;
+ higher resolution
- static system;
- complex optical alignment.

Ideal for dynamic studies and tomography

Which lenses to use to focus X-rays ?

Conrad Wilhelm Roentgen

When Roentgen discovered X-rays, he immediately tried to focus them with refractive lenses but did not succeed!

Why? …

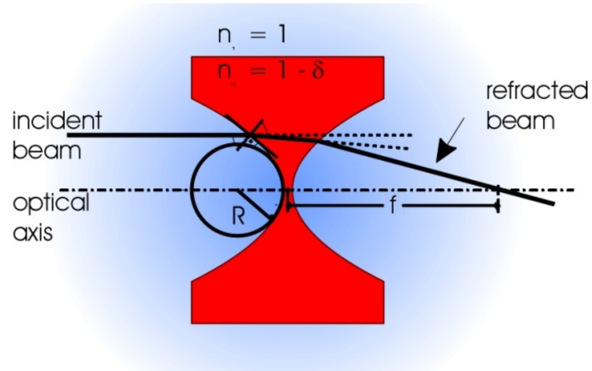

$$f = \frac{R}{2\delta}$$

For example: Al lens with R=500μm, E=10keV, $\delta = 5.46\ 10^{-6}$:

f = 92m

A reminder towards X-ray microscopy: The optics?

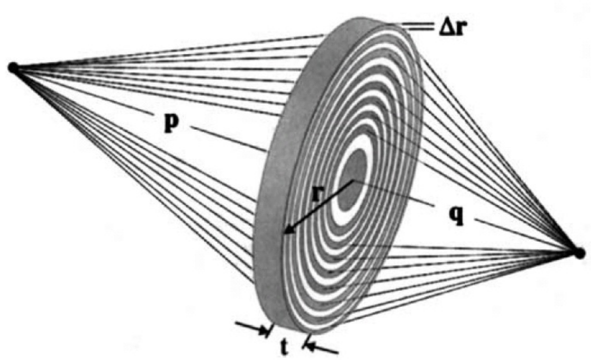

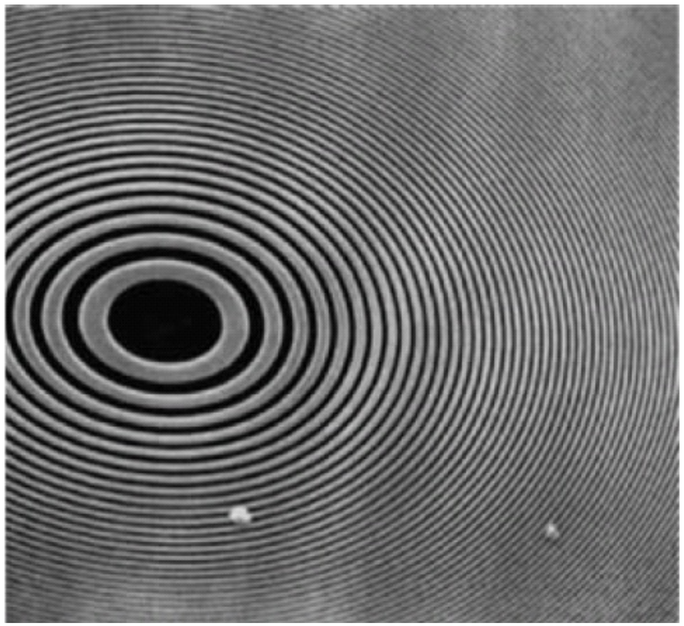

A zone plate (ZP) is a circular diffraction grating with radially increasing line density

$$\frac{1}{f} = \frac{1}{p} + \frac{1}{q} \quad \text{if } n > 100; \quad f = \frac{2r\Delta r}{\lambda}$$

Lateral resolution of a ZP (Rayleigh):

$$NA \equiv \frac{r}{f} = \frac{\lambda}{2\Delta r}$$

$$\partial_{Rayleigh} = \frac{0.61\lambda}{NA} = 1.22\Delta r$$

Background info: Diffraction by a grating

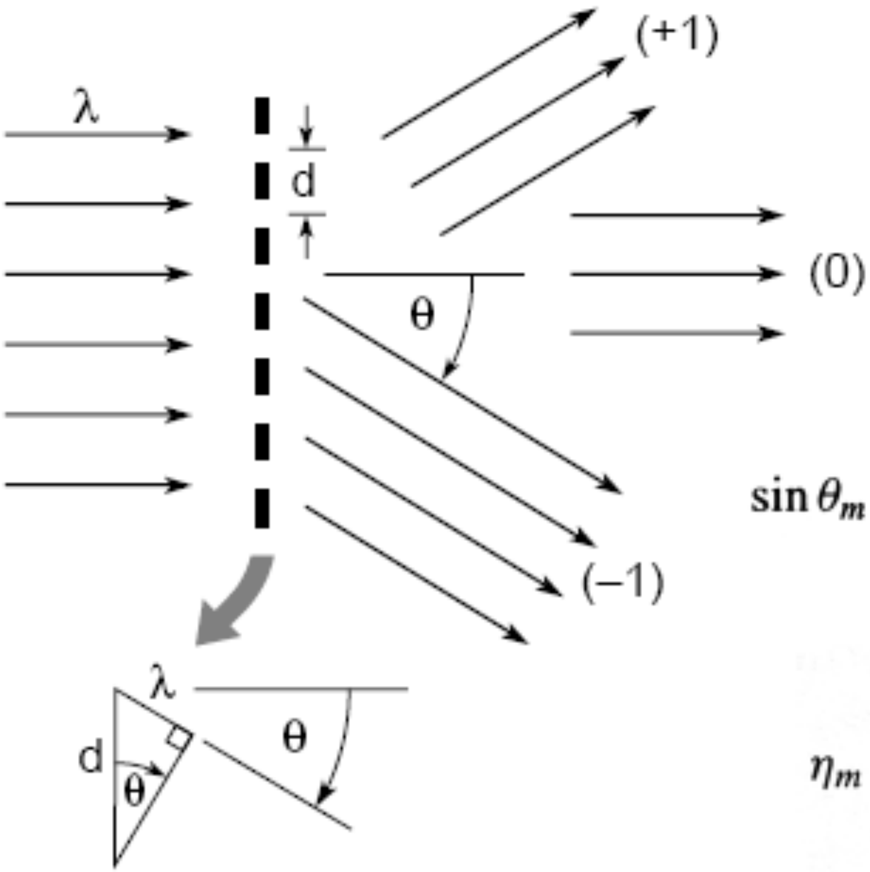

$$\sin\theta_m = \frac{m\lambda}{d}\,; \quad m = 0, \pm 1, \pm 2, \pm 3, \ldots \qquad (9.2)$$

$$\eta_m = \begin{cases} \frac{1}{4} & m = 0 \\ 1/m^2\pi^2 & m \text{ odd} \\ 0 & m \text{ even} \end{cases} \qquad (9.24)$$

(50% absorbed)

The transmission X-ray microscope (TXM) or full-field imaging microscope (FFIM)

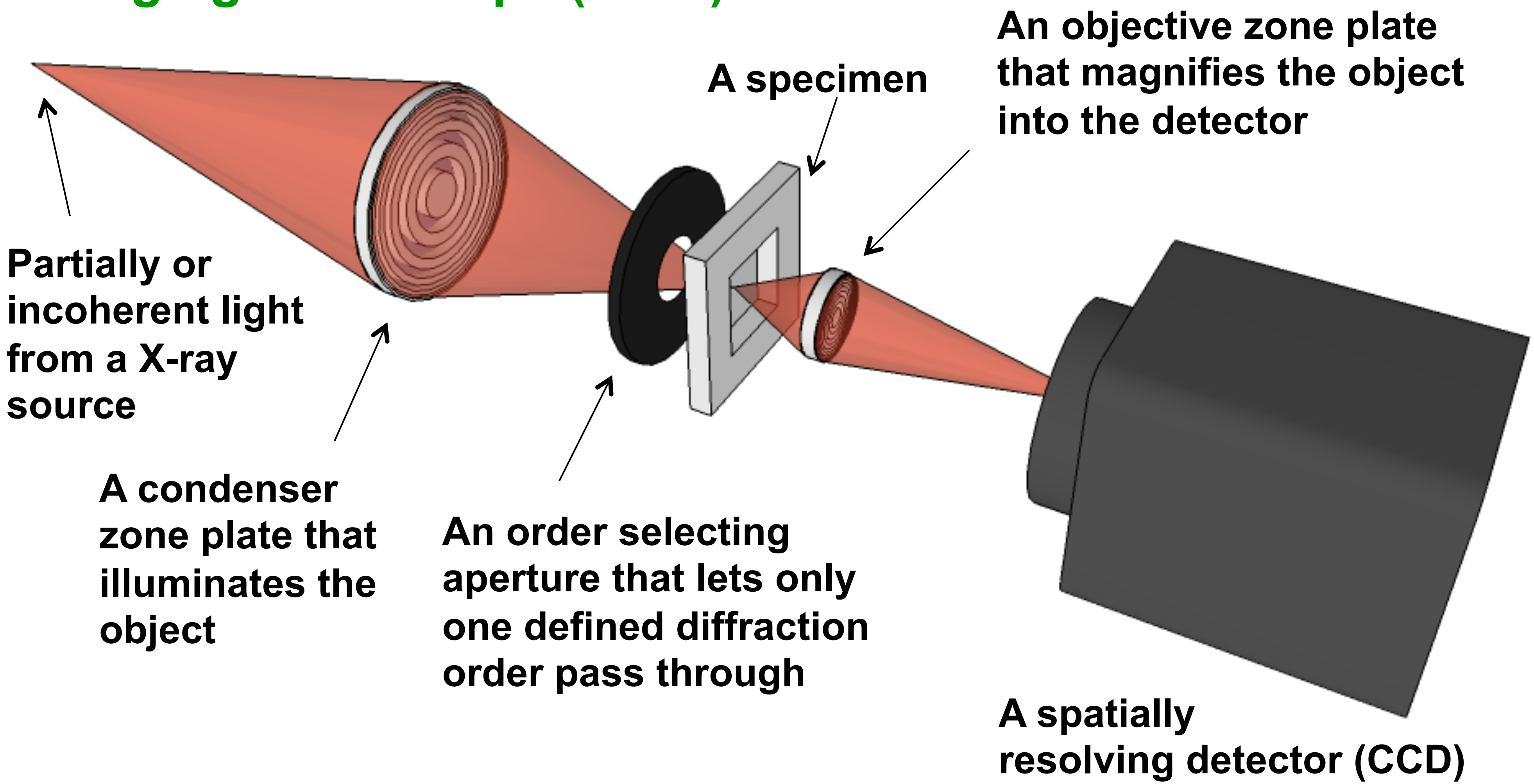

The XM-1 microscope at the ALS, LBL, CA, US:

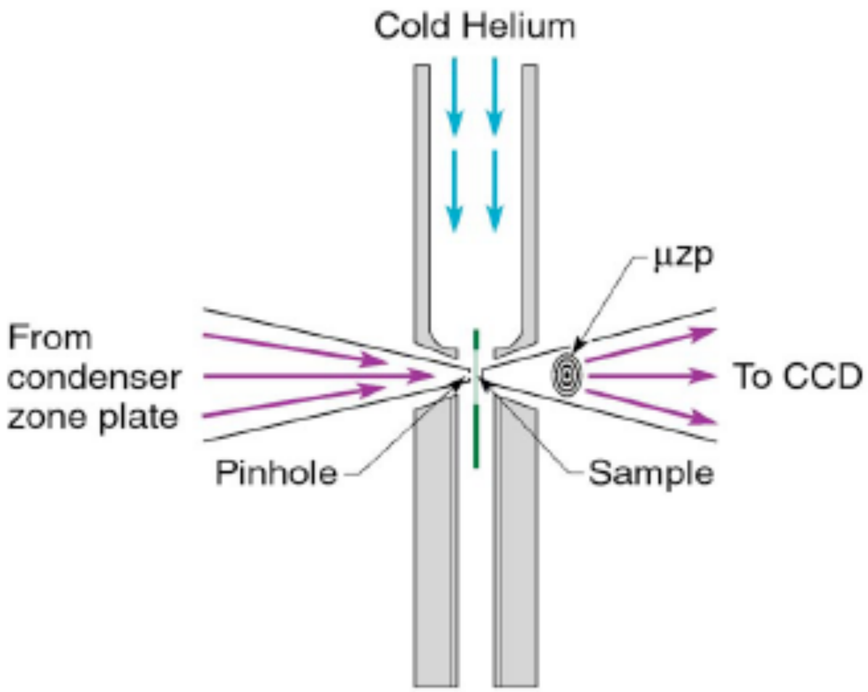

Helium passes through LN, is cooled, and directed onto sample windows

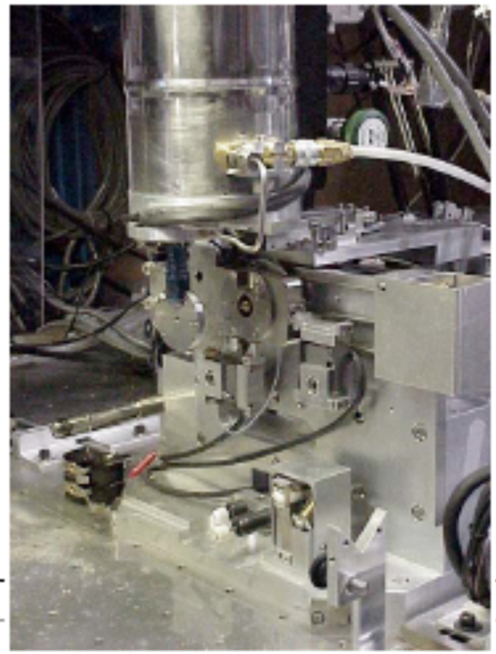

Fast Freeze

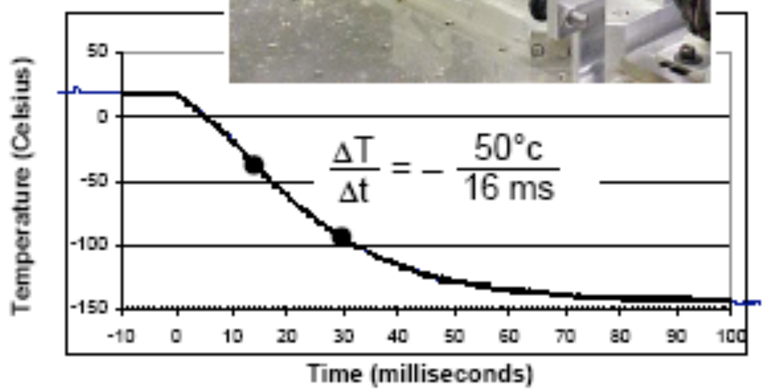

W. Meyer-Ilse, G. Denbeaux, L. Johnson, A. Pearson (CXRO-LBNL)

Natural amplitude contrast between water and organic matter

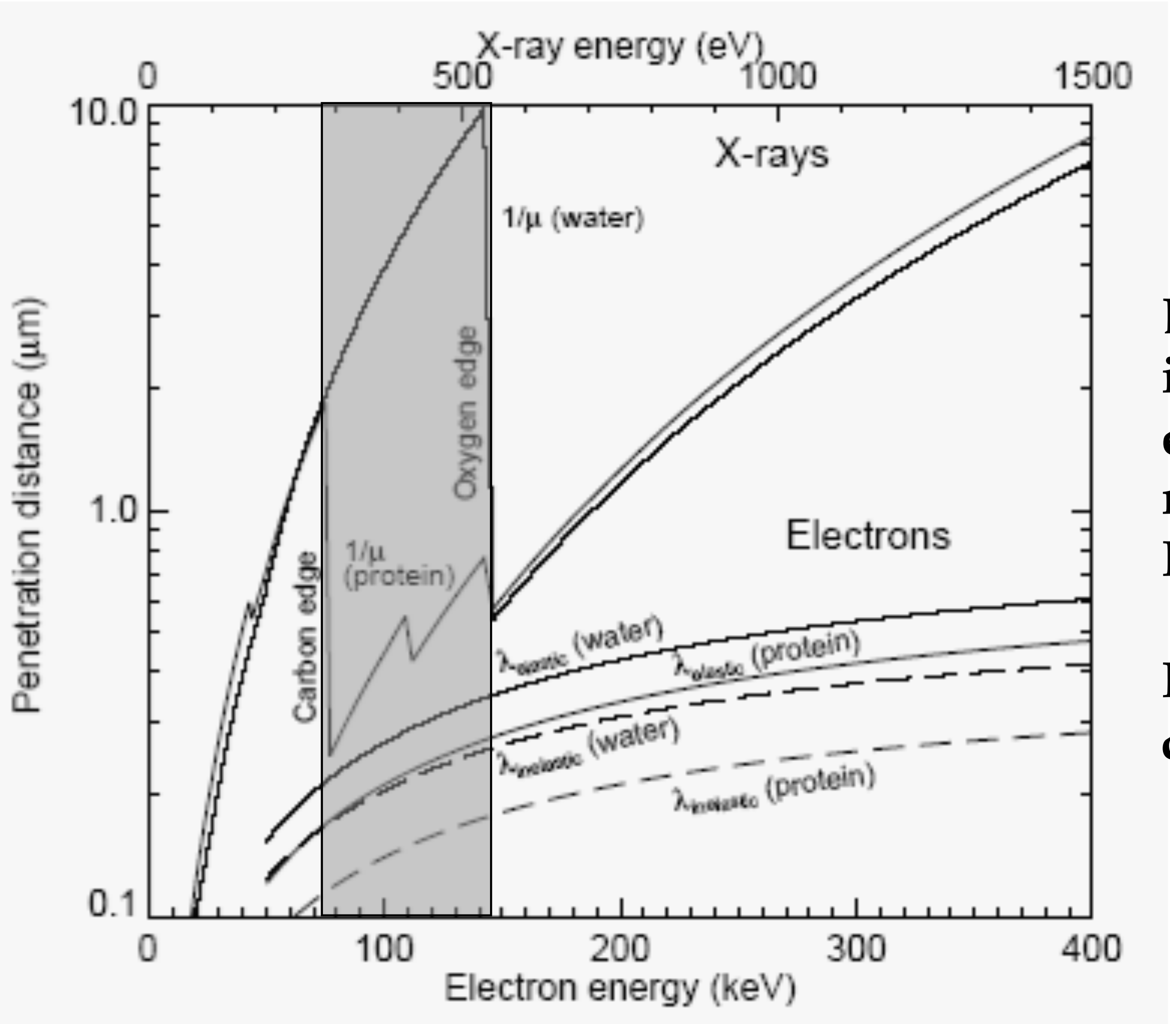

The "Water Window":

Due to dramatic difference in the f2 values of two materials, especially water and organic matter between the C and O K-absorption edges.

Note the penetration distance compared to electrons !!!

H. Wolter: ***Spiegelsysteme streifenden Einfalls als abbildende Optiken fuer Roentgenstrahlen***, **Ann. Phys. 10, 94-114, 286 (1952)**

Natural amplitude contrast between water and organic matter

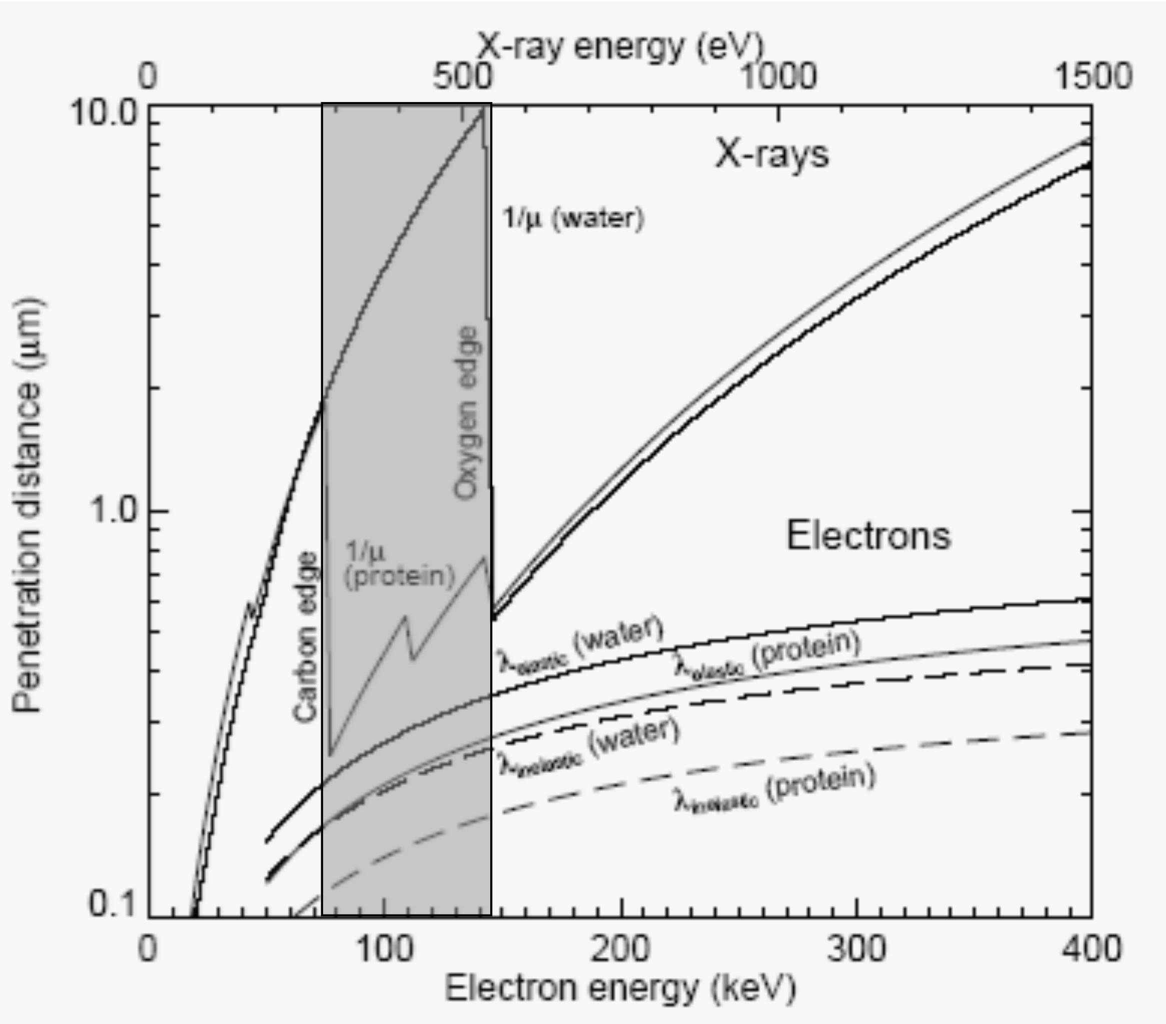

The "Water Window":

Organic matter absorbs approximately one order of magnitude more strongly than water

Chemical contrast agents are not required

H. Wolter: *Spiegelsysteme streifenden Einfalls als abbildende Optiken fuer Roentgenstrahlen*, Ann. Phys. 10, 94-114, 286 (1952)

The XM-1 microscope at the ALS, LBL, CA, US:

Cryo x-ray microscopy of 3T3 fibroblast cells

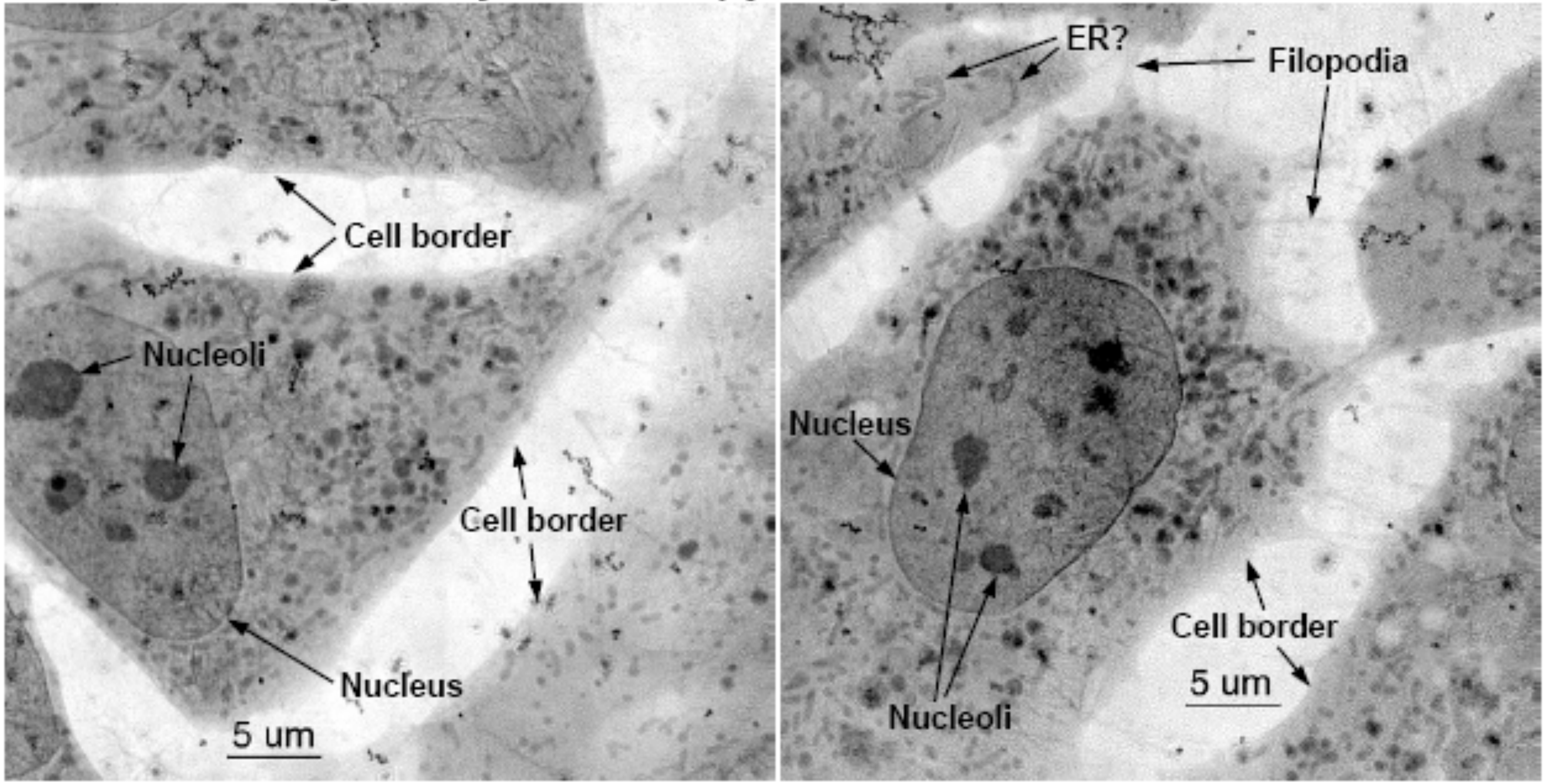

C. Larabell, D. Yager, D. Hamamoto, M. Bissell, T. Shin (LBNL Life Sciences Division)
W. Meyer-Ilse, G. Denbeaux, L. Johnson, A. Pearson (CXRO-LBNL)

E=517 eV

Major full-field imaging instruments for biological applications

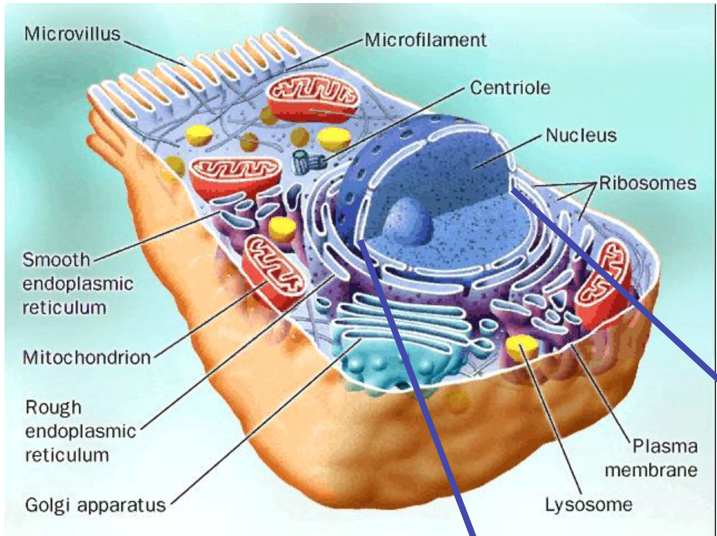

Location of Splicing Factors in whole, hydrated human mammary epithelial Cells (ALS, XM1)

Rapidly frozen samples

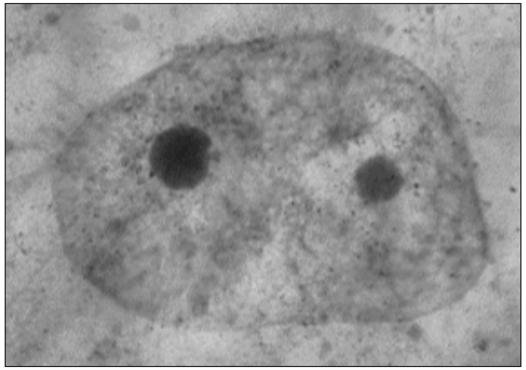

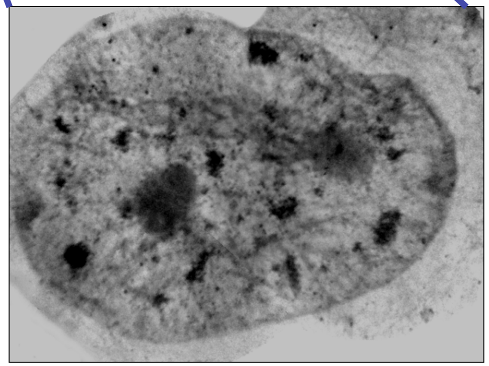

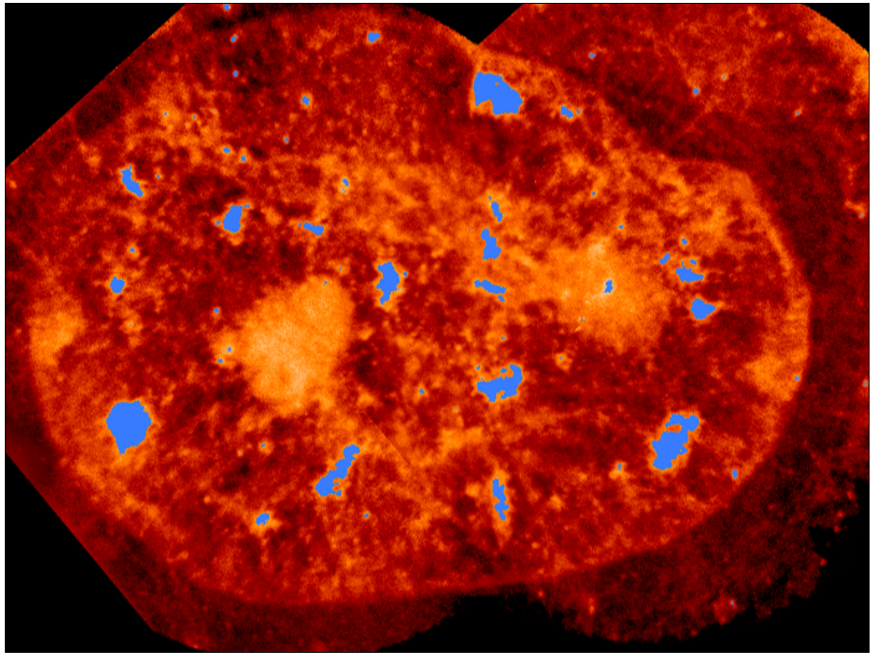

Control nucleus, no primary antibody

Single nucleus labeled using antibodies specific for splicing factors

Same nucleus, splicing factors colored blue

Resolution better than 50nm

Image courtesy: C. Larabell, LBL, US

Meyer-Ile et al. Journal of Microscopy, 201, 395-403 (2001)

The XM-1 microscope at the ALS, LBL, CA, US:

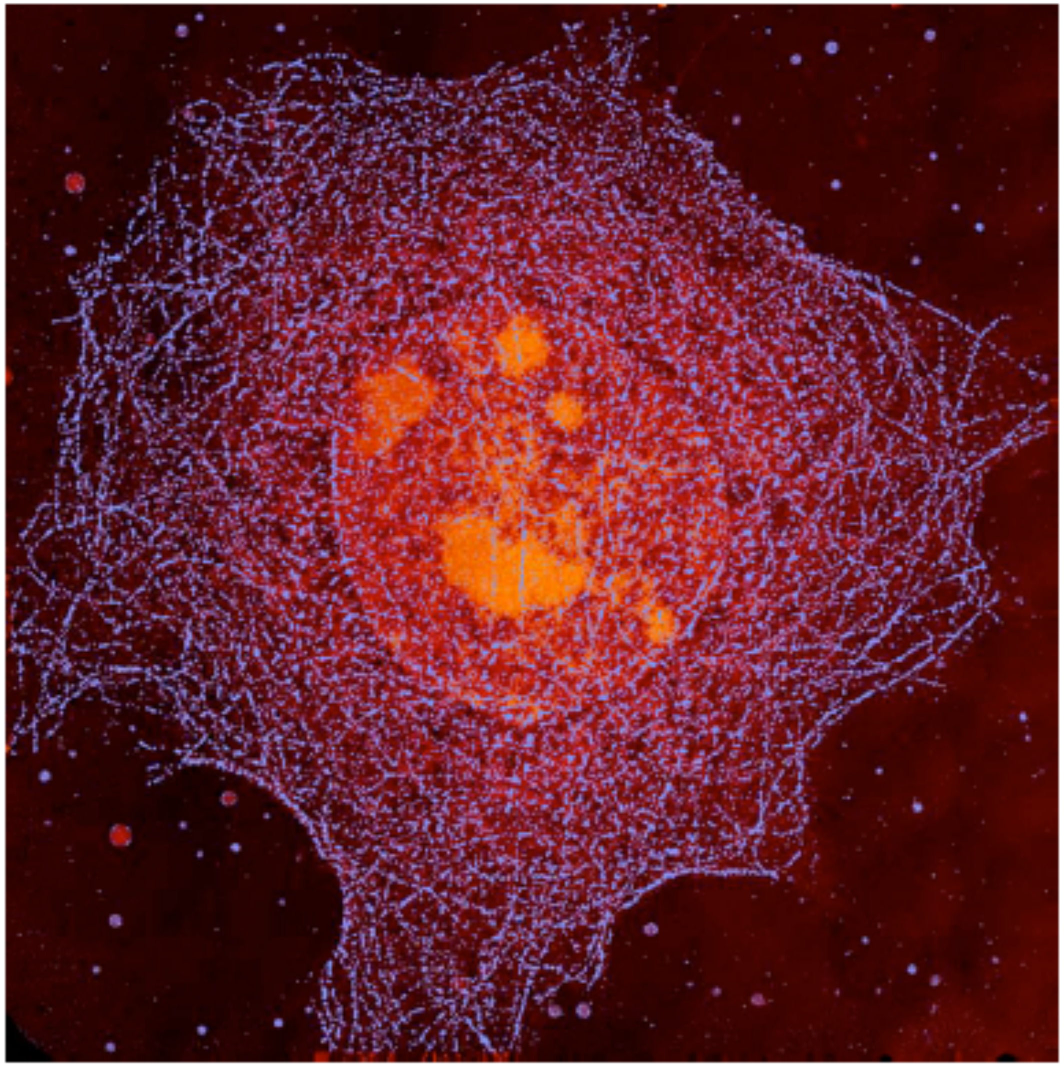

Courtesy of C. Larabell and W. Meyer-Ilse (LBNL)

Localization of proteins by utilizing gold-labelled antibodies

$\hbar w = 520$ eV

32 μm x 32 μm

Ag enhanced Au labeling of the microtubule network, color coded blue.

Cell nucleus and nucleoli, moderately absorbing, coded orange.

Less absorbing aqueous regions coded black.

W. Meyer-Ilse et al.
J. Microsc. 201, 395 (2001)

Cryogenic 3D imaging of biological cells

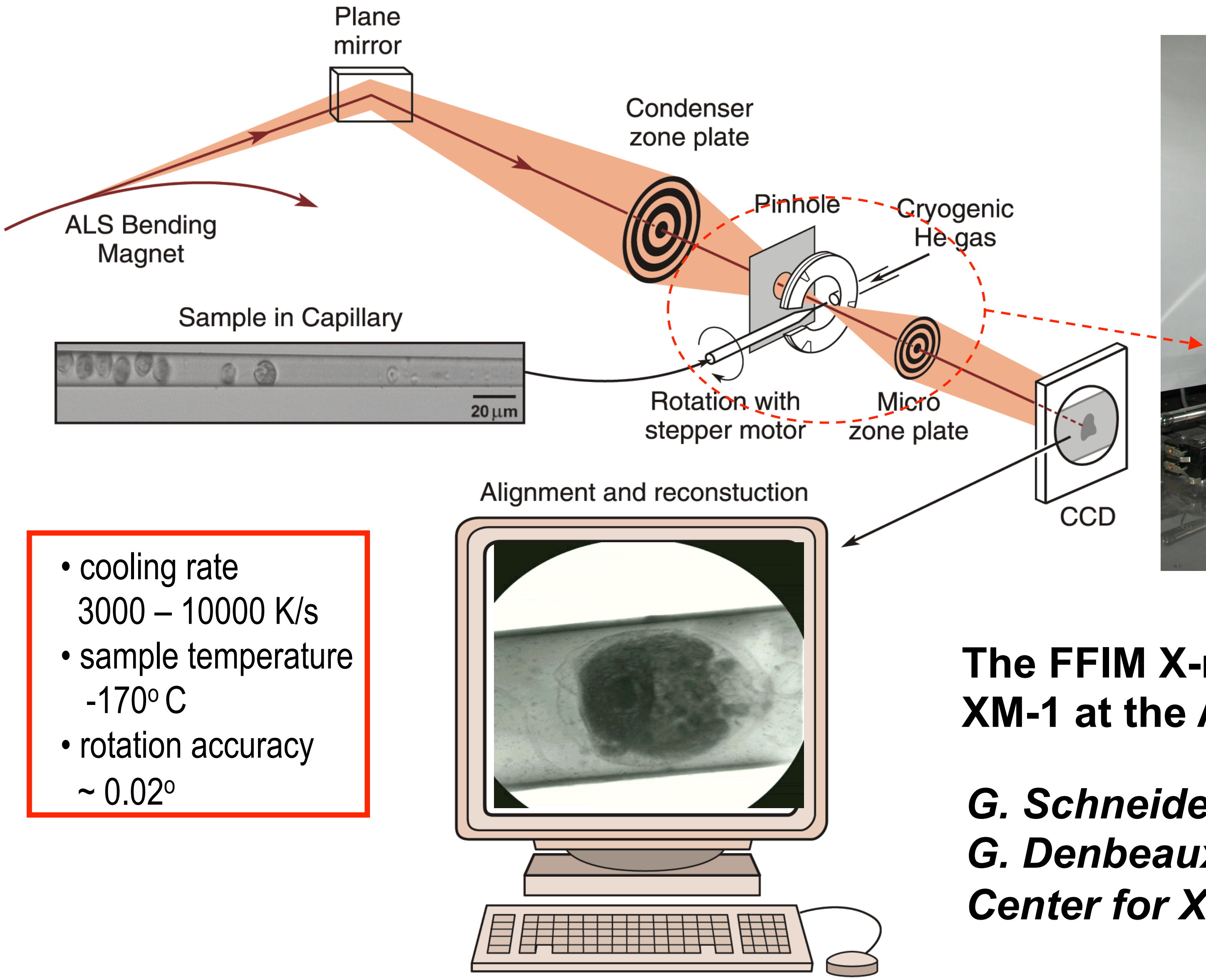

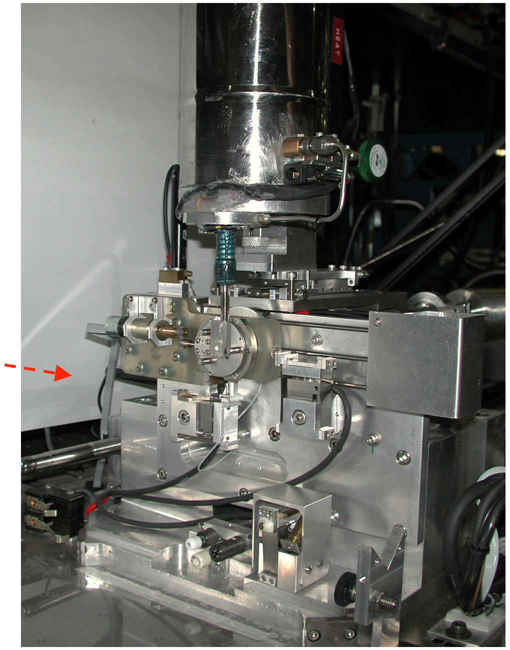

- cooling rate 3000 – 10000 K/s
- sample temperature -170° C
- rotation accuracy ~ 0.02°

The FFIM X-ray microscope XM-1 at the ALS, CA, USA

G. Schneider, B. Bates, G. Denbeaux, E. Anderson, Center for X-ray Optics, LBL

Cryogenic 3D imaging of biological cells

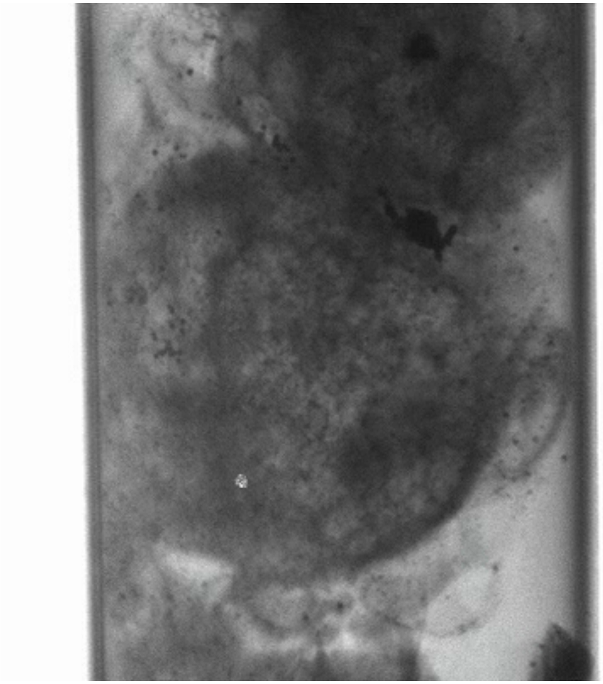

FFIM micrographs of a specimen in the capillary

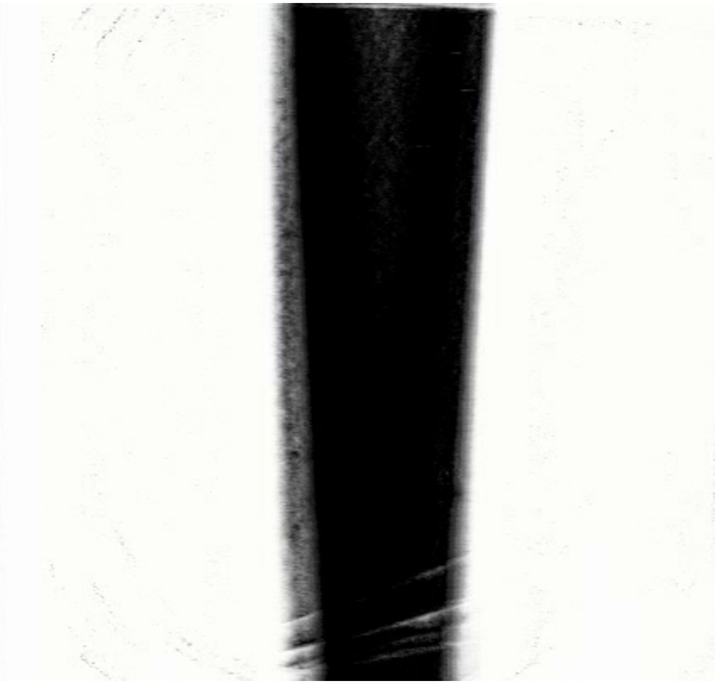

Reconstructed sections through the volume

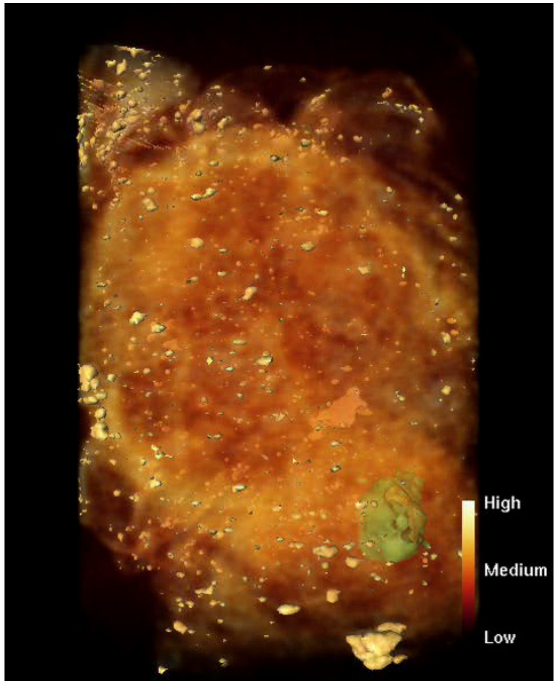

Reconstruction of the absorption coefficient

Work performed with the XM1 microscope at the ALS, US (G. Schneider, G. Denbeaux, B. Bates and E. Anderson)

The XM-2 microscope at the ALS, LBL, CA, US National Center for X-ray Tomography:

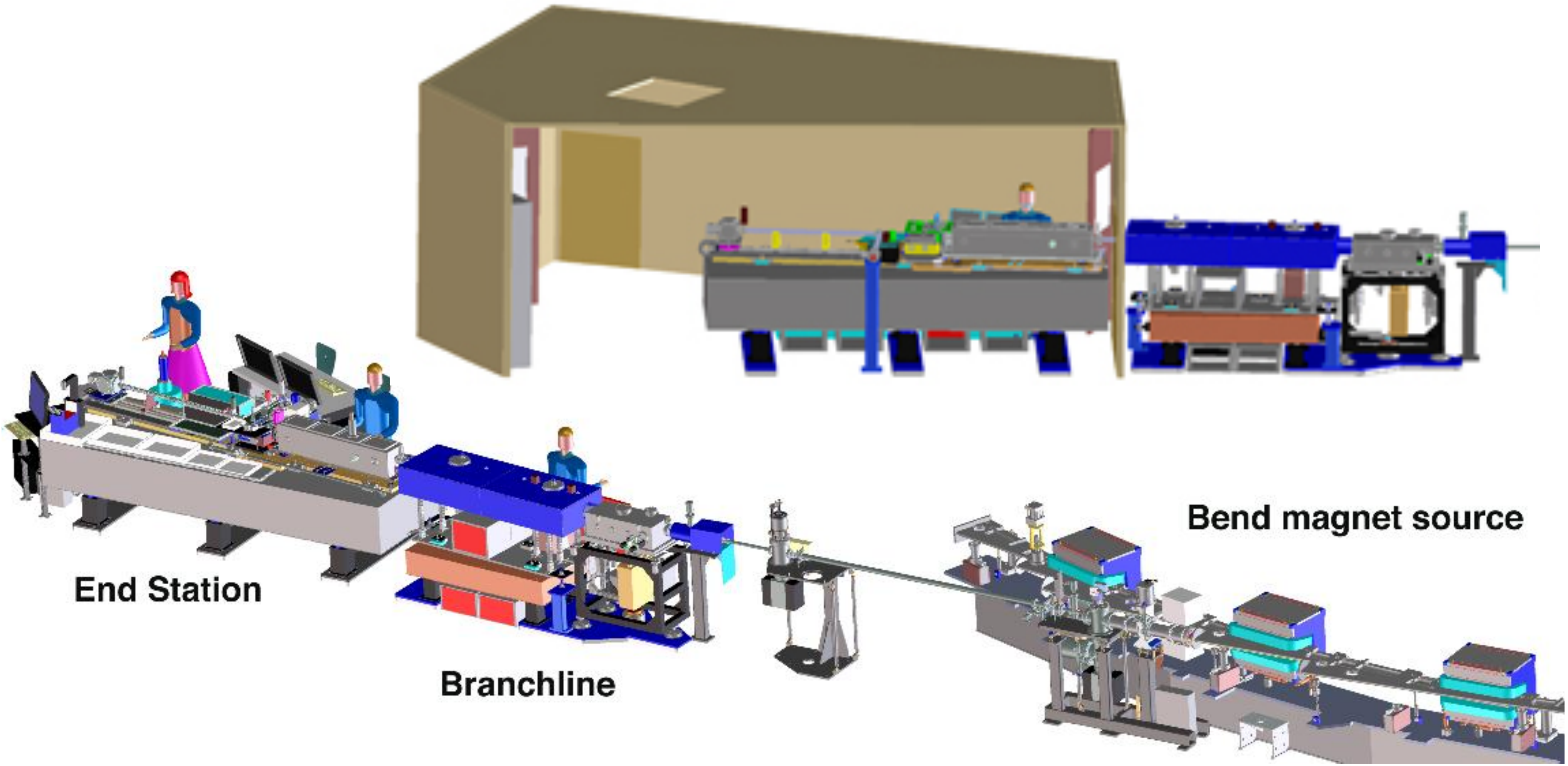

The XM-2 microscope at the ALS, LBL, CA, US
National Center for X-ray Tomography:

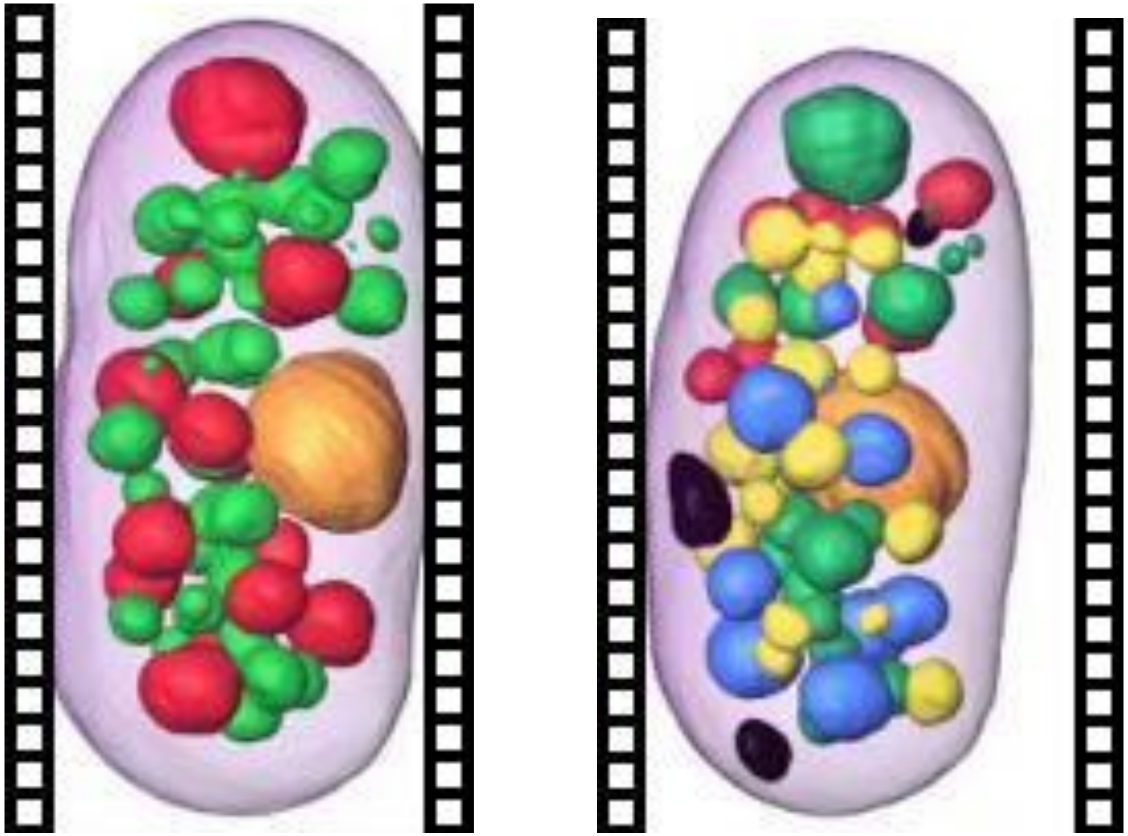

3D reconstructions of S. pombe cells; early stage cell segmentation (left) and early stage mitochondria and vacuoles (right)

Visit http:www.ncxt.lbl.gov to see the movies

The full-field imaging microscope at BESSY II, Berlin, Germany:

http://www.bessy.de

Cryogenic 3D imaging of biological cells

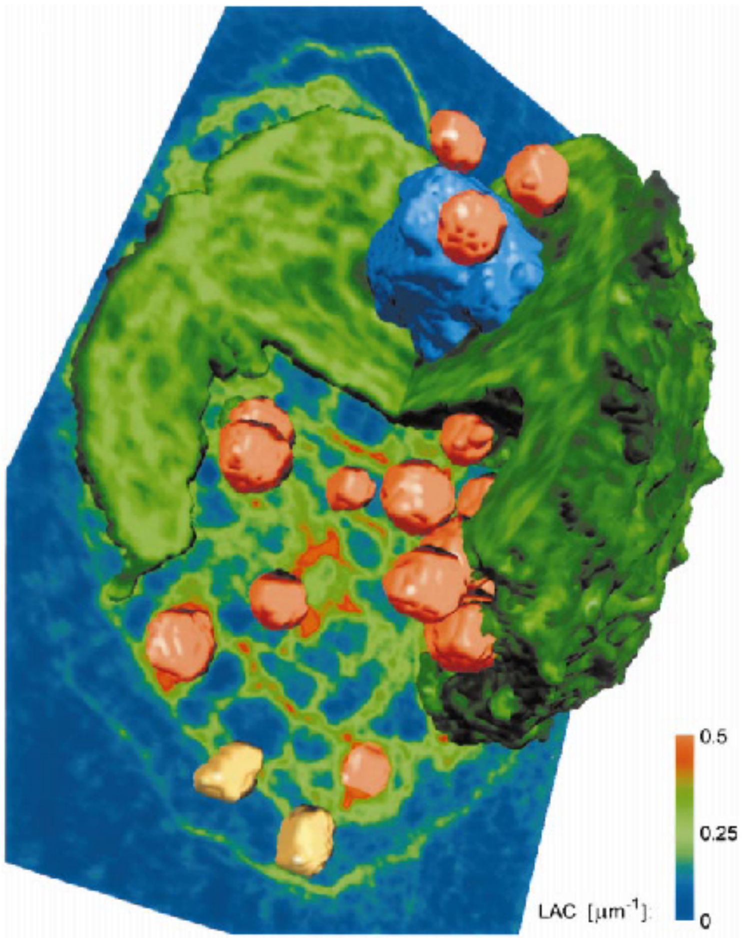

X-ray tomography of hydrated specimen "close to their living state"

Alga: Chlamydomonas reinhardtii

Acquired with the full-field imaging Microscope at BESSY I

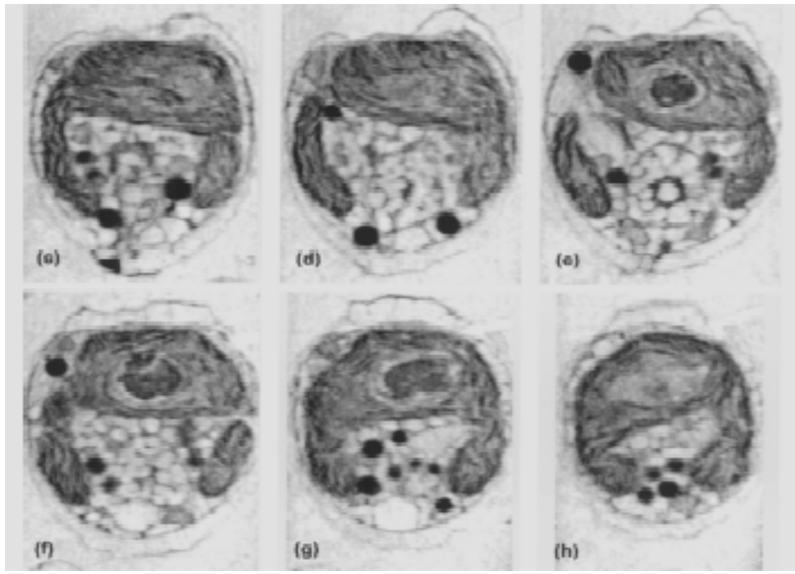

Image courtesy: D. Weiss et al., BESSY, D

Environmental science: Imaging in liquids

Bacteria and clay dispersion: Destruction of associations of clay particles by soil microbes

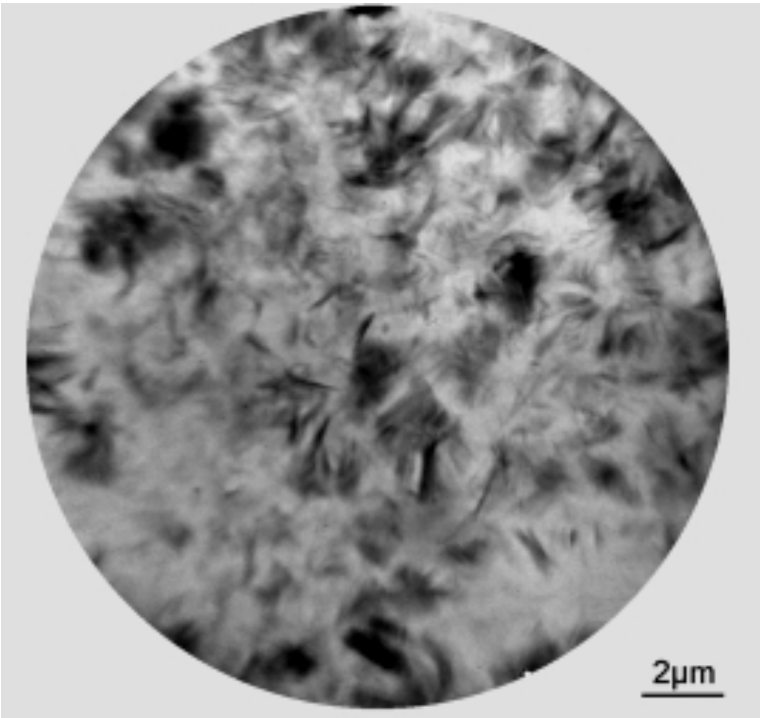

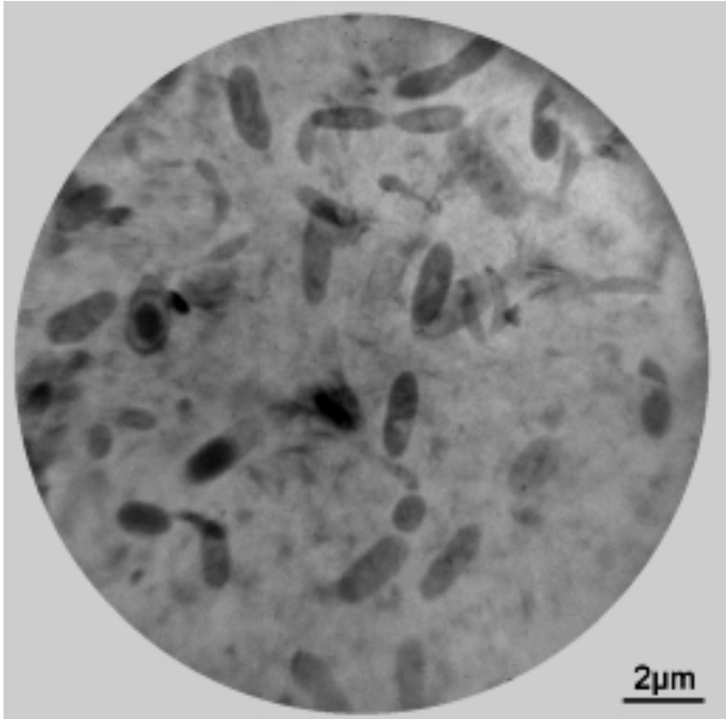

X-ray images acquired with the full-field imaging microscope at BESSY I @ 520 eV

Samples analysed in the natural hydrated state:
→ no alteration of the environment of the sample

J. Thieme et al., IRP, Uni Goettingen / G. Machulla, Uni Halle, D

Across edge imaging

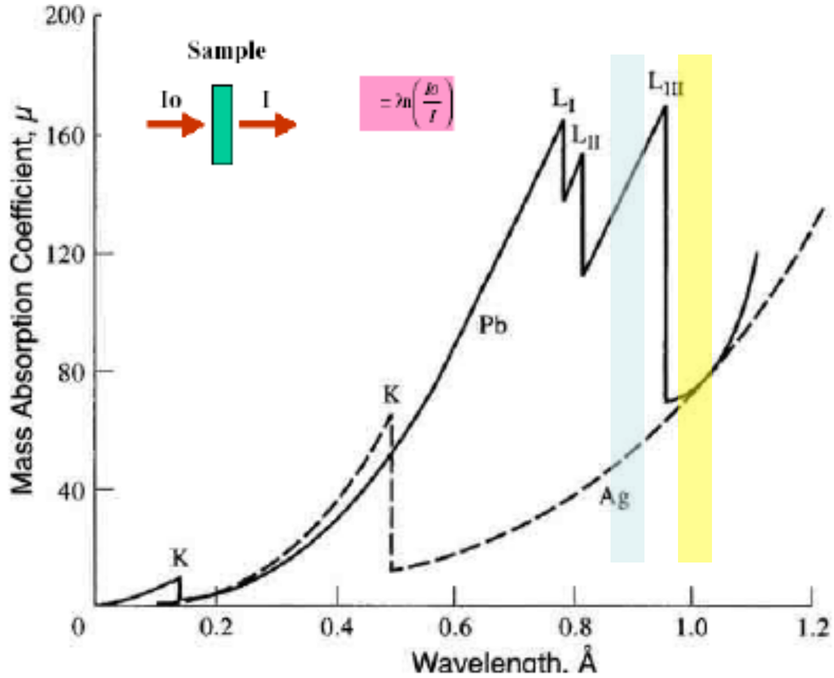

Discontinuities due to absorption

The absorption occures when the incoming X-rays are matching the electron binding energies

Absorption edges are fingerprints ⇒ they can be used to identify the chemical elements

By taking two images, one above and one below a specific absorption edge, the correspondent chemical element will give a high contrast difference in the two images

Across edge imaging

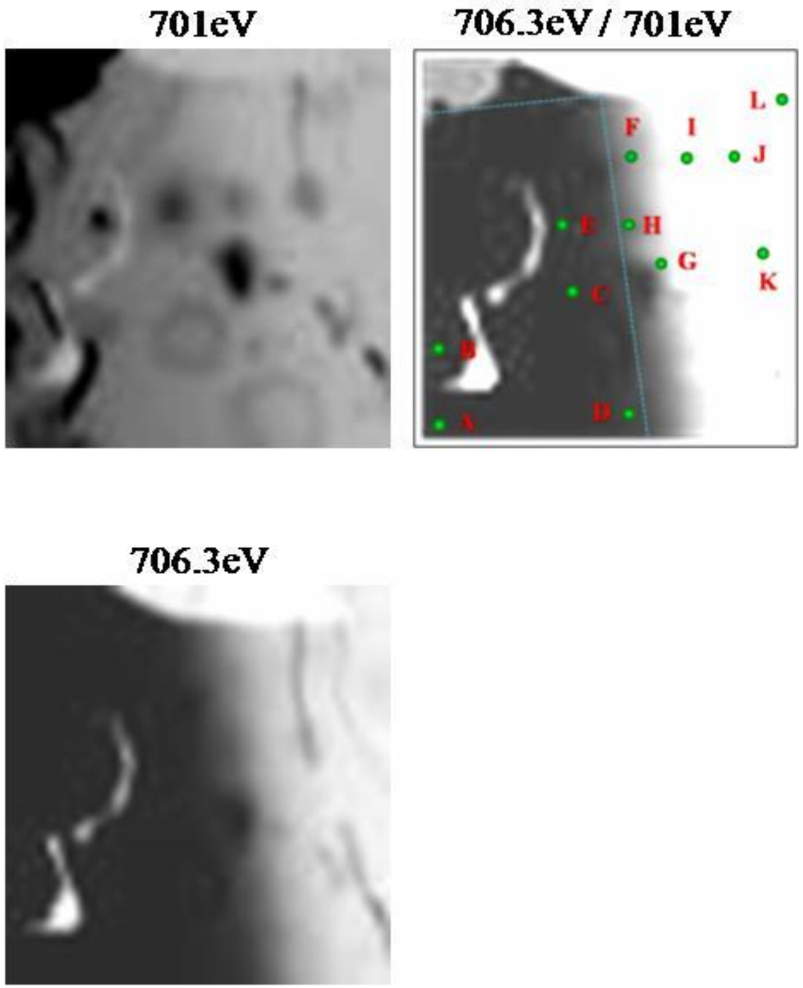

B. Bozzini, A. Gianoncelli, B. Kaulich, .M. Kiskinova, M. Prasciolu, I. Sgura, Metallic Plate Corrosion and Uptake of Corrosion Products by Nafion in Polymer Electrolyte Membrane Fuel Cells, ChemSusCHem 2010, 3, 846-850.

Environmental science: Analysis of air particulate matter

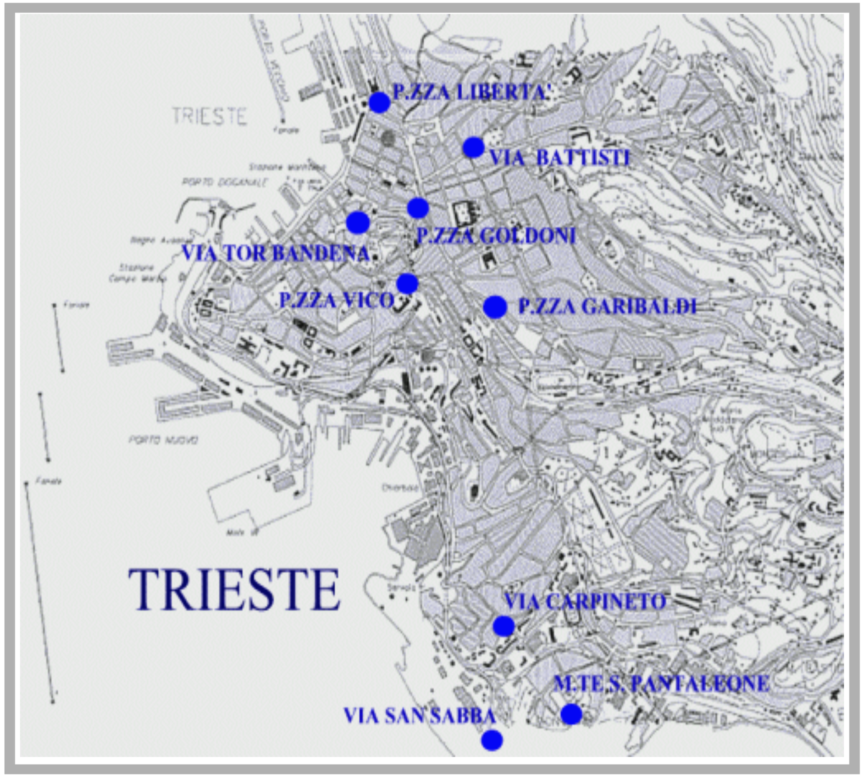

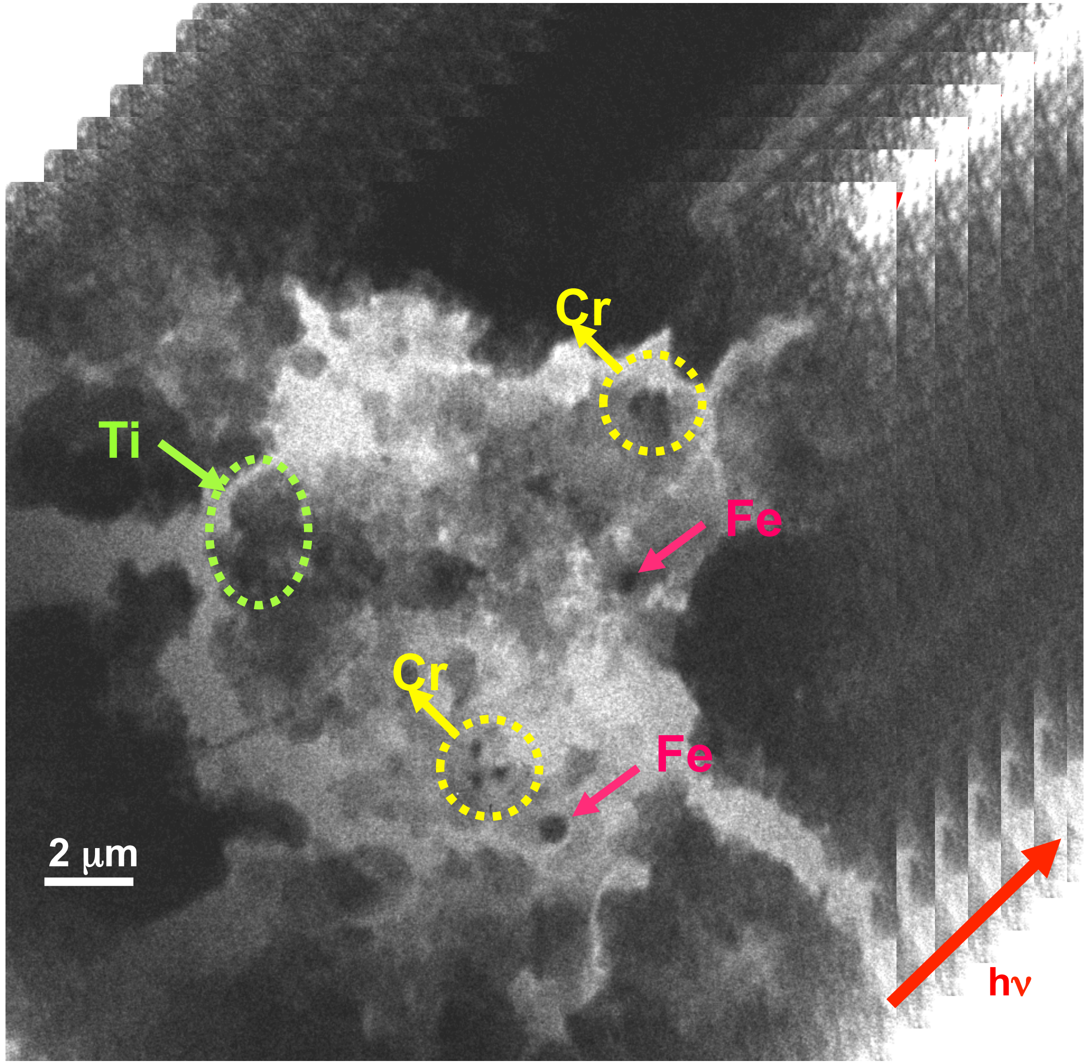

P. Barbieri et al.,
Dept. of Chem., Univ. Trieste, I

Phase contrast techniques are well established in microscopies, especially for low-absorbing specimen (as in life sciences)

Can we apply phase-sensitive imaging techniques in transmission X-ray microscopy?

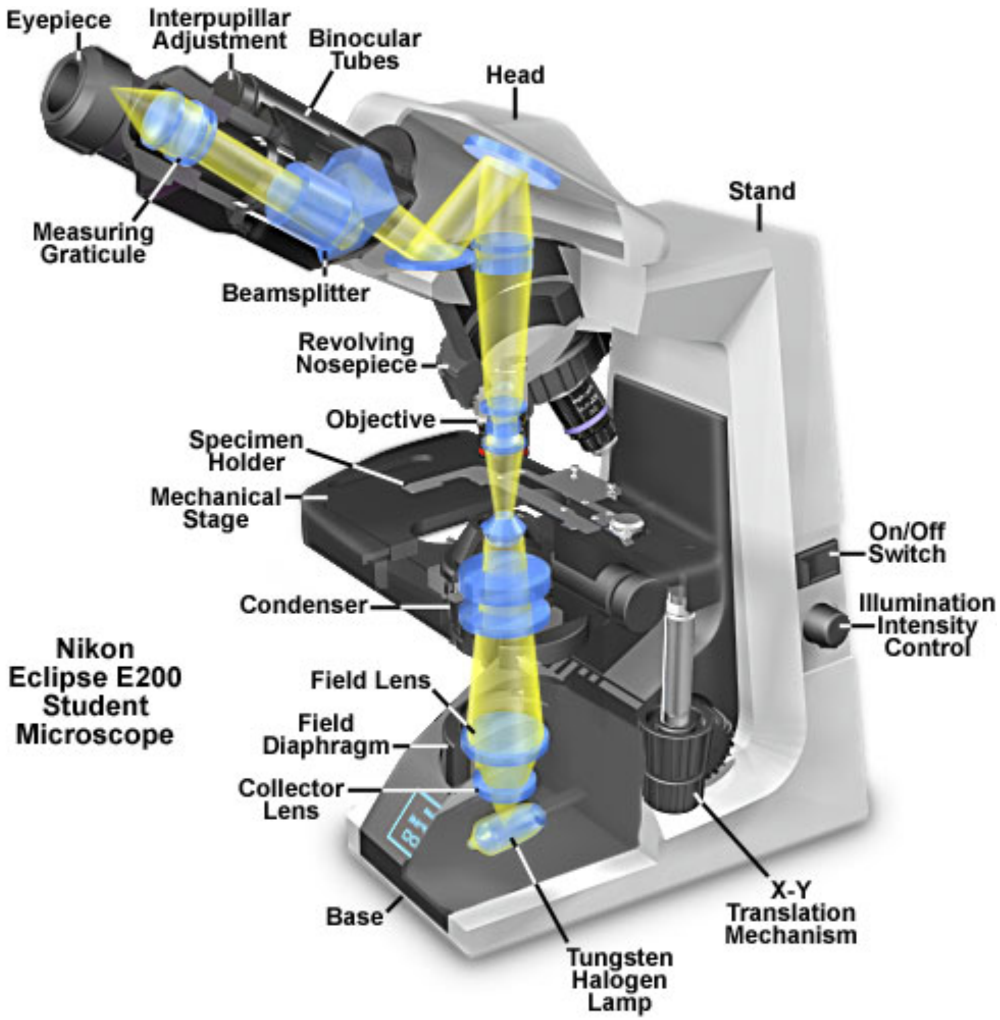

Cutaway diagram of a visible light microscope

Full-field X-ray imaging or "one shot" X-ray image acquisition can be considered as the optical analogon to a visible light transmission microscope

BUT

Refractive index n is very close to unity and smaller than unity!!!

$$n = 1 - \delta(\lambda) - i\beta(\lambda) < 1$$

The complex refractive index

$$n = 1 - \frac{n_a r_e \lambda^2}{\pi}\left(f_1 + i f_2\right) \equiv 1 - \delta - i\beta \leq 1$$

"Conventional refractive index" describing phase change:

$$\varphi(z) = \frac{2\pi}{\lambda}\delta z$$

Exploitation of phase contrasts possible using X-rays ?
Lower radiation damage ?

Describing photoelectric absorption with coefficient:

$$\mu = \frac{4\pi}{\lambda}\beta$$

Consequence:
Emission of Auger, photo-electrons and fluorescence photons, but also causes radiation damage (energetic secondary electrons!)

Refractive index and X-ray contrast techniques

X-ray contrast is generated by *differences* in the complex scattering factor per unit volume

$$n(\lambda) = 1 - \delta(\lambda) - i\beta(\lambda) = 1 - \frac{n_a r_e \lambda^2}{2\pi}\left(f_1(\lambda) - f_2(\lambda)\right)$$

$$\delta(\lambda) = \frac{n_a r_e \lambda^2}{2\pi} f_1(\lambda)$$

$$\beta(\lambda) = \frac{n_a r_e \lambda^2}{2\pi} f_2(\lambda)$$

$\delta(\lambda)$: Phase sensitive
$\beta(\lambda)$: Absorption …
n_a: average atom density
r_e: classical electron radius
f_1, f_2: atomic form factors

Scattering, refraction:

- Zernike phase contrast
- Differential phase contrast
- Differential interference contrast
- Dark-field imaging
- Magnetic phase contrast

Absorption:

- Bright-field imaging
- Chemical contrast techniques
- Magnetic absorption contrast

Delta versus beta

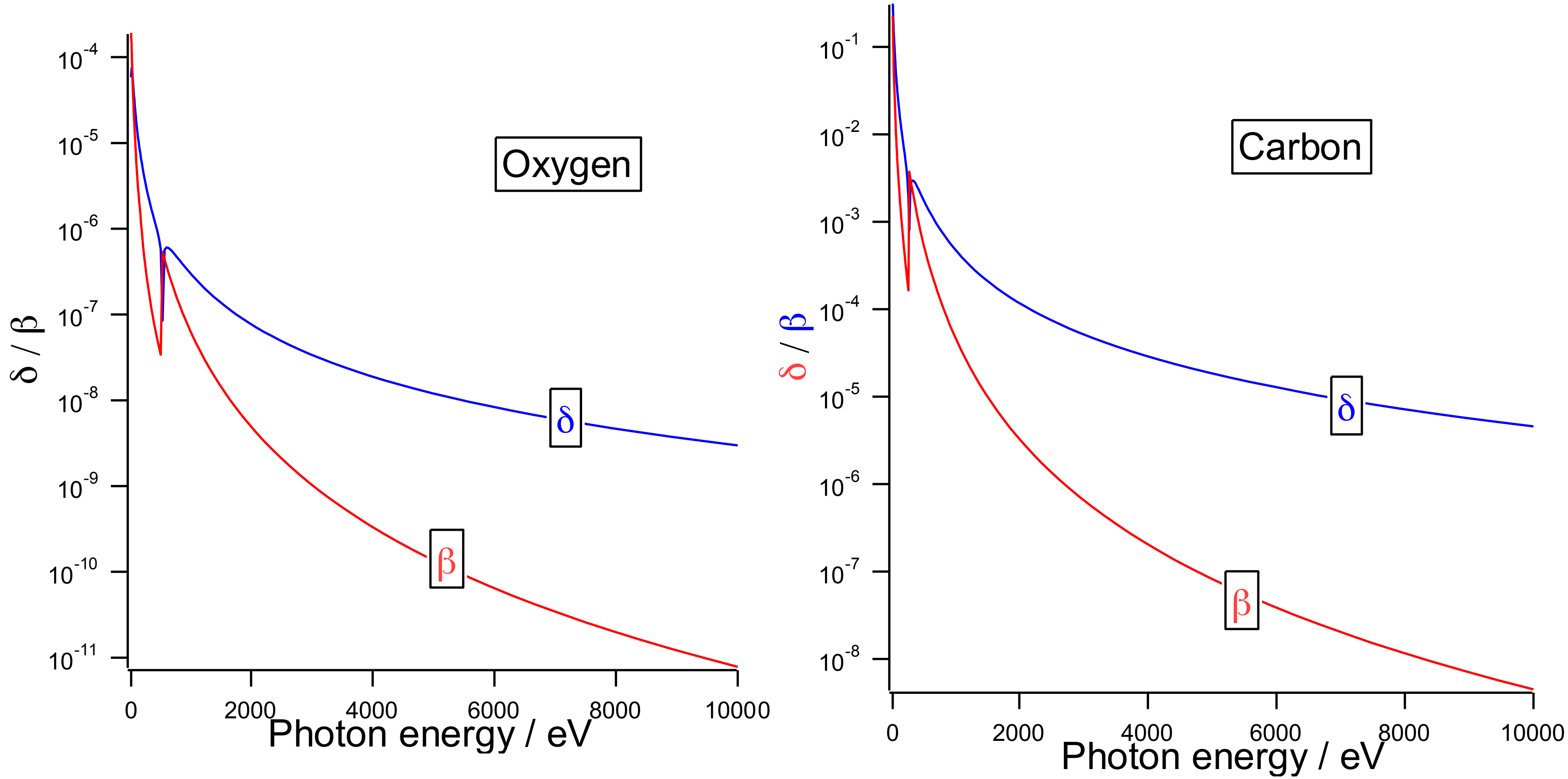

Delta is orders of magnitude larger !!!

Absorption mode

X-ray photons are selectively absorbed by the material according to its density and thickness
(ex. radiography)

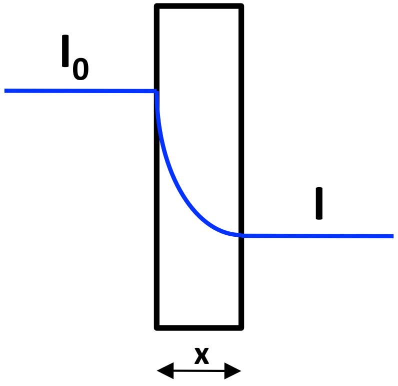

Beer - Lambert's law:
$I = I_0 e^{-mx}$

Phase contrast mode

Absorption can produce little contrast for light (transparent) materials or for materials with similar atomic number (similar attenuation factors).

Moreover as the energy increases the contrast diminishes (absorption coefficient $\propto 1/E^3$)

Phase contrast is more sensitive to edges and borders in the sample

Contrast techniques using the real, phase-shifting part of the complex refractive index are in many cases superior to absorption contrast because:
(i) the x-ray dose can be reduced dramatically
(ii) the throughput is higher (the phase shift dominates the absorption in the x-ray regime)

B. Kaulich et al. J. Phys.: Condens. Matter 23 (2011) 083002

Definition of contrast

Often applied definition:

Contrast is defined as the difference in light intensity between the image and the adjacent background relative to the overall background intensity

$$C = 100 \cdot \frac{(I_S - I_B)}{I_B}$$

I_s: Specimen intensity
I_b: Background intensity

Definition used for XRM:

Contrast is defined as the difference in maximum and minimum light intensity normalized to the sum of maximum and minimum light intensity

$$C = \frac{(I_{\max} - I_{\min})}{I_{\max} + I_{\min}}$$

I_{max}: Max. image intensity
I_{min}: Min. image intensity

Absorption versa phase contrast techniques

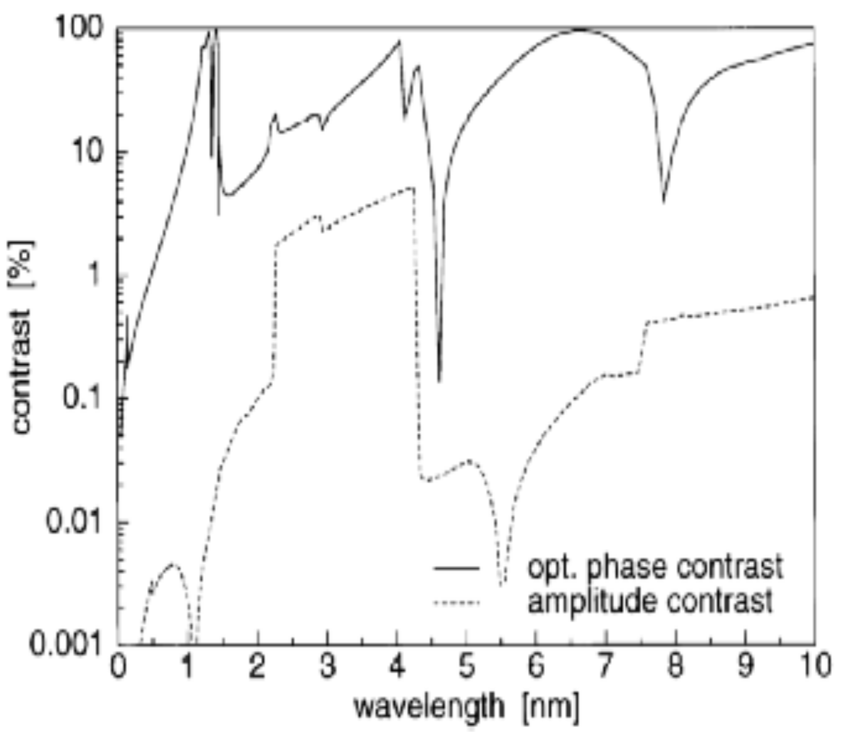

Amplitude and phase contrast for a model protein $C_{94}H_{139}N_{24}O_{31}$

Courtesy of G. Schneider et al. BESSY, D

Absorption contrast

Mostly used for chemical studies in combination with XANES and XRF

Phase contrast techniques

- **tremendous reduction of dose applied to object (dose ~ t^{-4} with spat. resolution t)**
- **additional transmission information on low side of absorption edges (XANES, XRF !)**

Full field Imaging mode

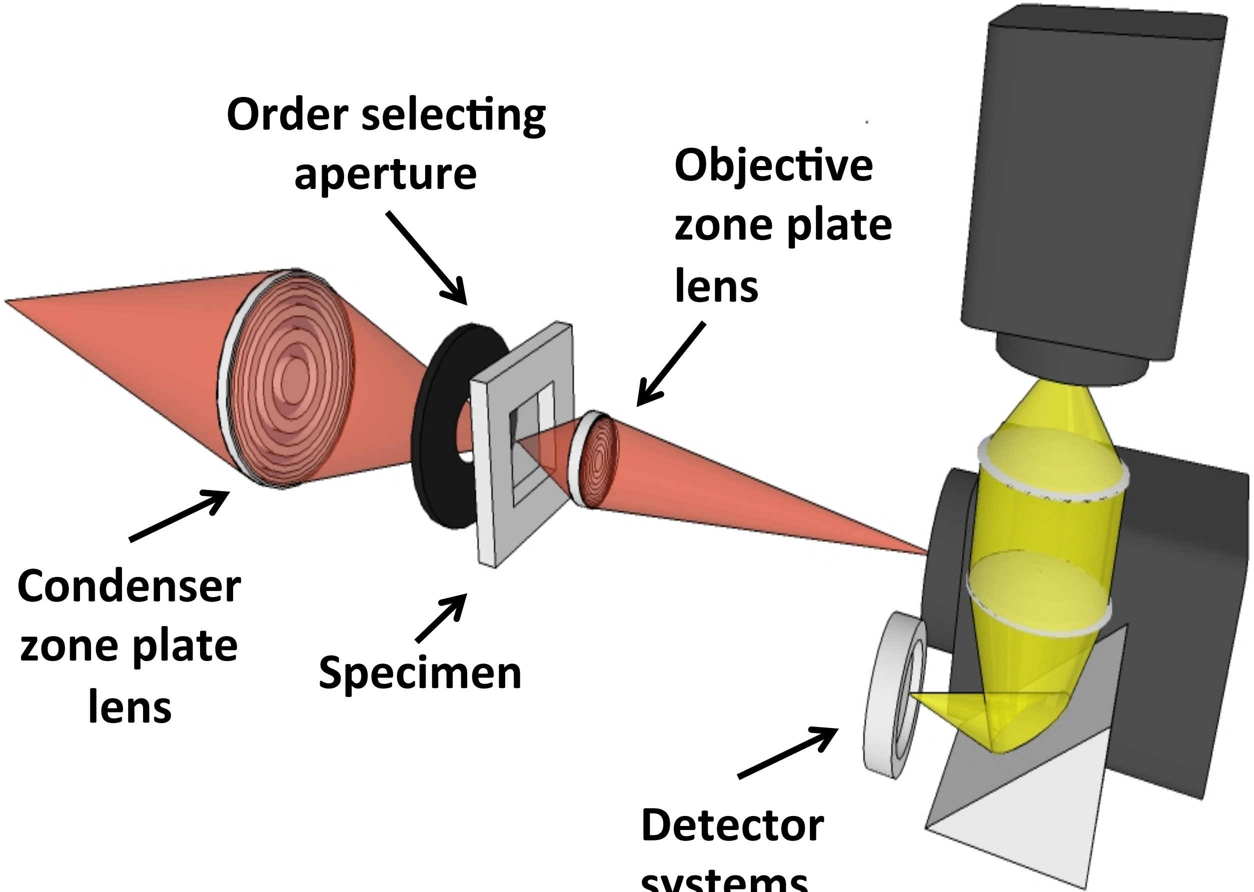

- Similar to conventional visible light microscope
- Analysis of morphology in transmission
- Fast imaging, dynamics, microtomography

Basics of Zernike phase contrast

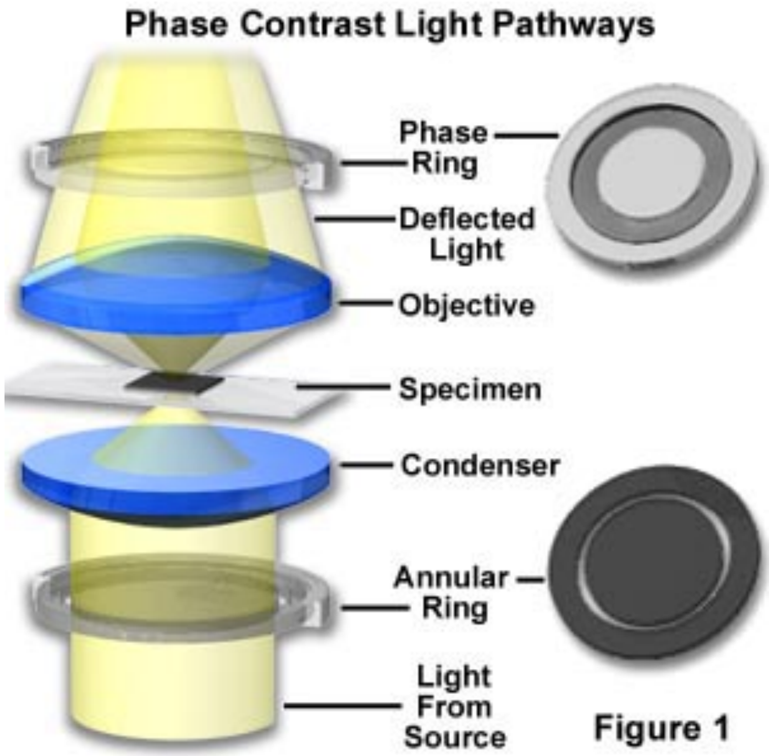

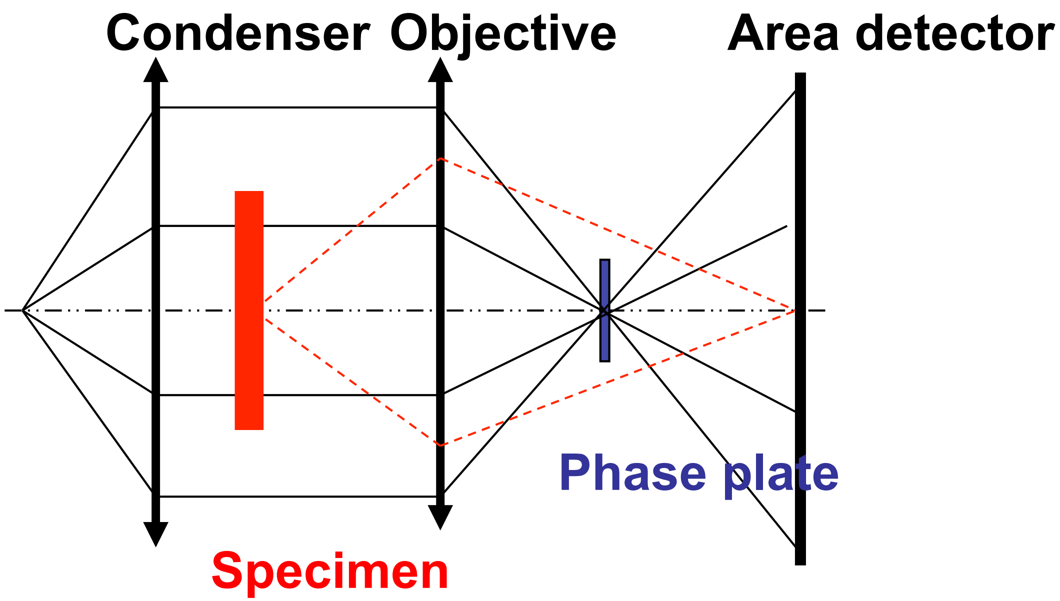

$$A_{specimen} = A_{surr} e^{i\Phi} = A_{surr} e^{i\frac{2\pi}{\lambda}\Delta t} \approx A_{surr}(1 + i\Phi) \qquad \Phi << 1$$

For imaging weakly absorbing samples

Phase plate in "back-focal" plane: Phase of A_{surr} can be shifted by +/- $\pi/2$!!!
Phase differences are converted in amplitude differences !!!

Zernike phase contrast in full-field imaging X-ray microscopy

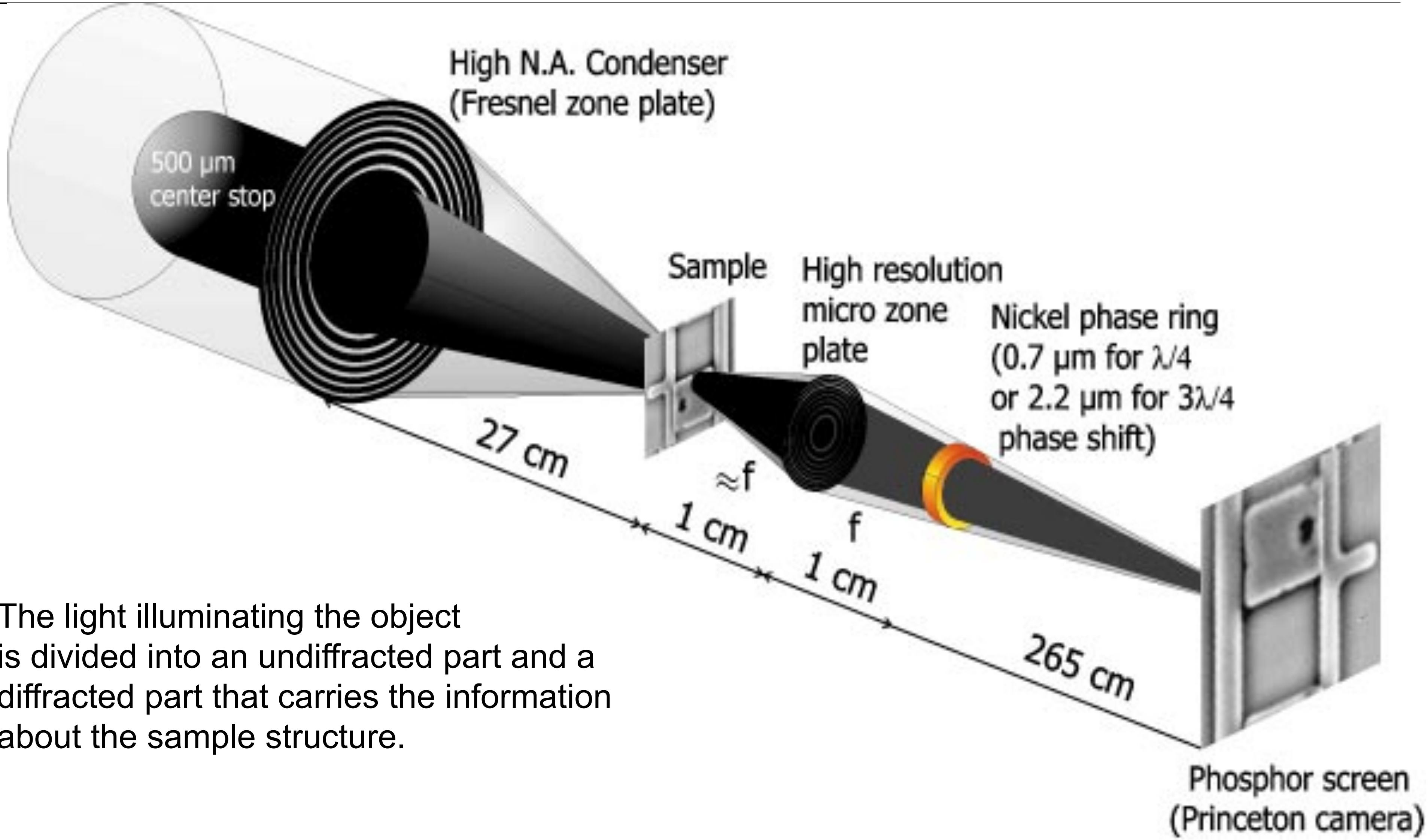

The light illuminating the object
is divided into an undiffracted part and a
diffracted part that carries the information
about the sample structure.

Zernike phase contrast in full-field imaging X-ray microscopy

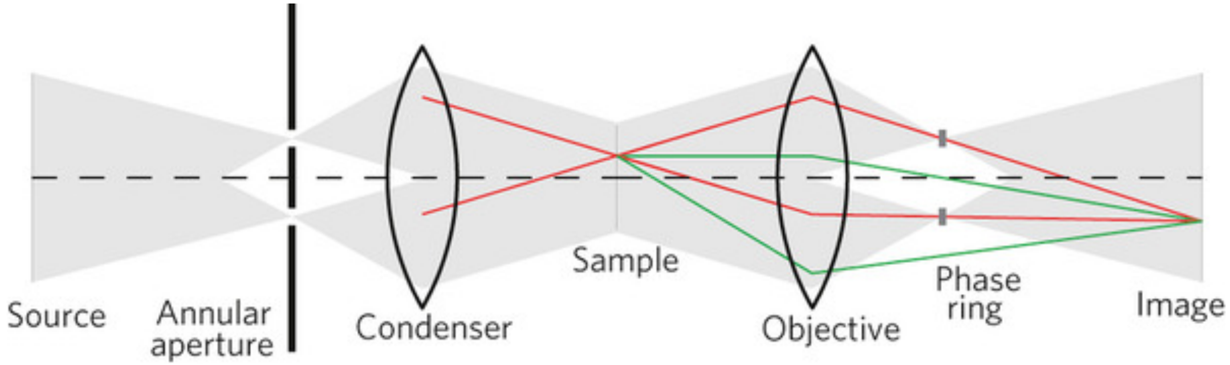

- The light illuminating the object is divided into an undiffracted part and a diffracted part that carries the information about the sample structure.
- A spatial separation of these two components is achieved in the back-focal plane of the objective lens, where a phase-shifting ring imparts a predetermined phase shift (90° for positive contrast or 270° for negative contrast) onto the undiffracted part.
- The phase-contrast image is formed by the interference of the phase-shifted undiffracted component with the undisturbed diffracted component, translating phase modulations of the sample into intensity modulations in the image plane.
- For small phase shifts, these modulations are due to the differences in the real part of the object's index of refraction, whereas the imaginary part leading to absorption contrast is usually small and can often be neglected.

C. Holzner et al. ***Nature Physics*** **6**, 883–887 (2010)

TXM images of S. cerevisiae at 5.4 keV

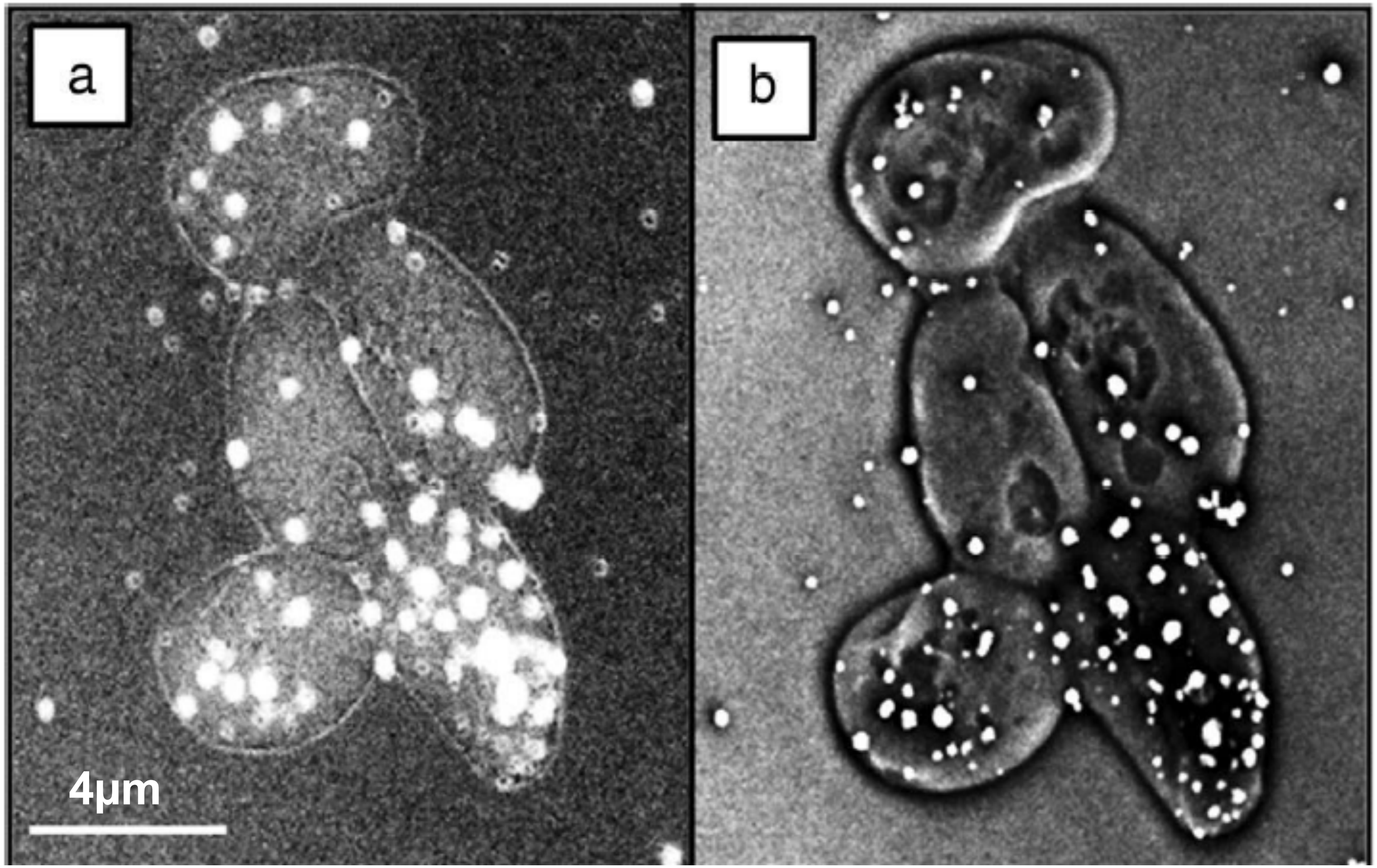

a) in absorption contrast **(b) in Zernike phase contrast**

J. C. Andrews et al. Microscopy Research and Technique 74: 671-681 (2011)

Zernike phase contrast in X-ray microscopy

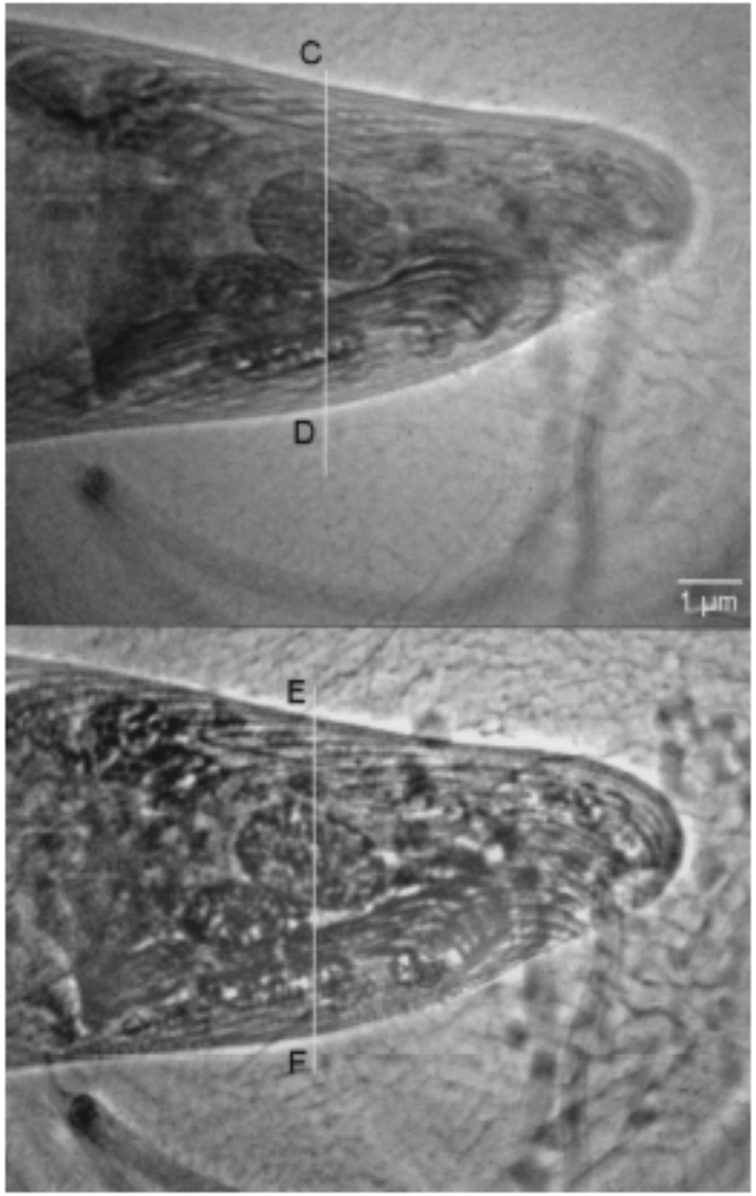

Amplitude and Zernike phase contrast images of an alga *Euglena gracilis*

E = 500 eV, accumulated dose is 3×10^6 Gray

Amplitude: 3 s
Phase contrast: 15 s

Drawbacks of Zernike phase contrast:

- **Halos around structures**
- **Quantitative analysis difficult**
- **Limitation in spatial resolution**
- **Not all spatial frequencies are treated equally**

Schneider et al. (1998) Proceedings 5th XRM, Springler, Thieme et al. Eds, I-111

Darkfield or darkground imaging

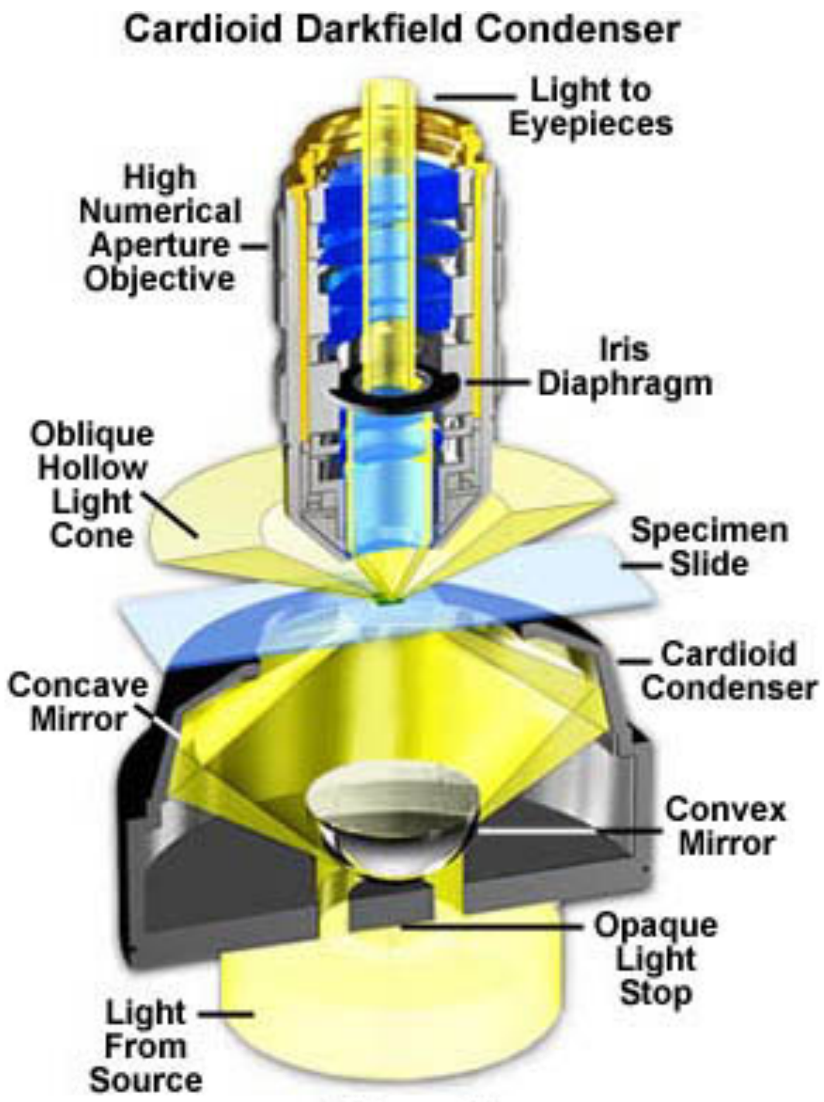

Figure 1

Darkfield illumination requires blocking out of the central light which ordinarily passes through and around (surrounding) the specimen, allowing only oblique rays from every azimuth to "strike" the specimen.

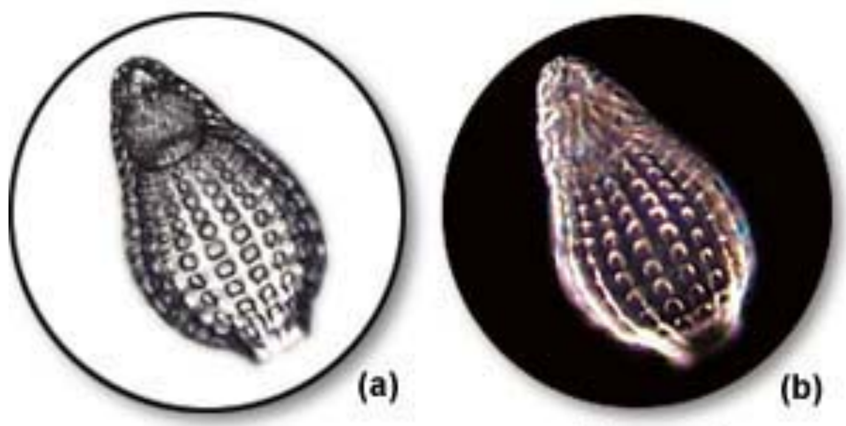

Visible light micrographs of silica skeletons from a small marine protozoan (radiolarian)

Darkfield imaging in scanning X-ray microscopy

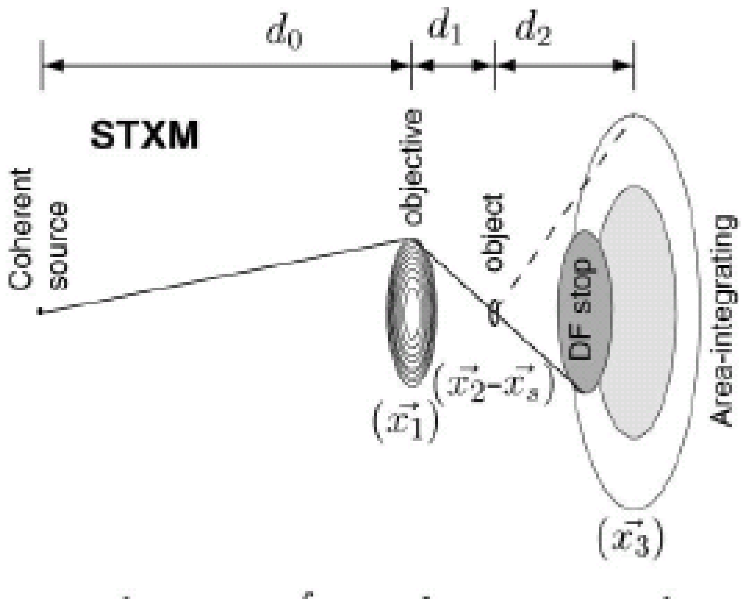

Technique is especially suited for small, strongly scattering particles as for example a few 10nm diameter labelling spheres

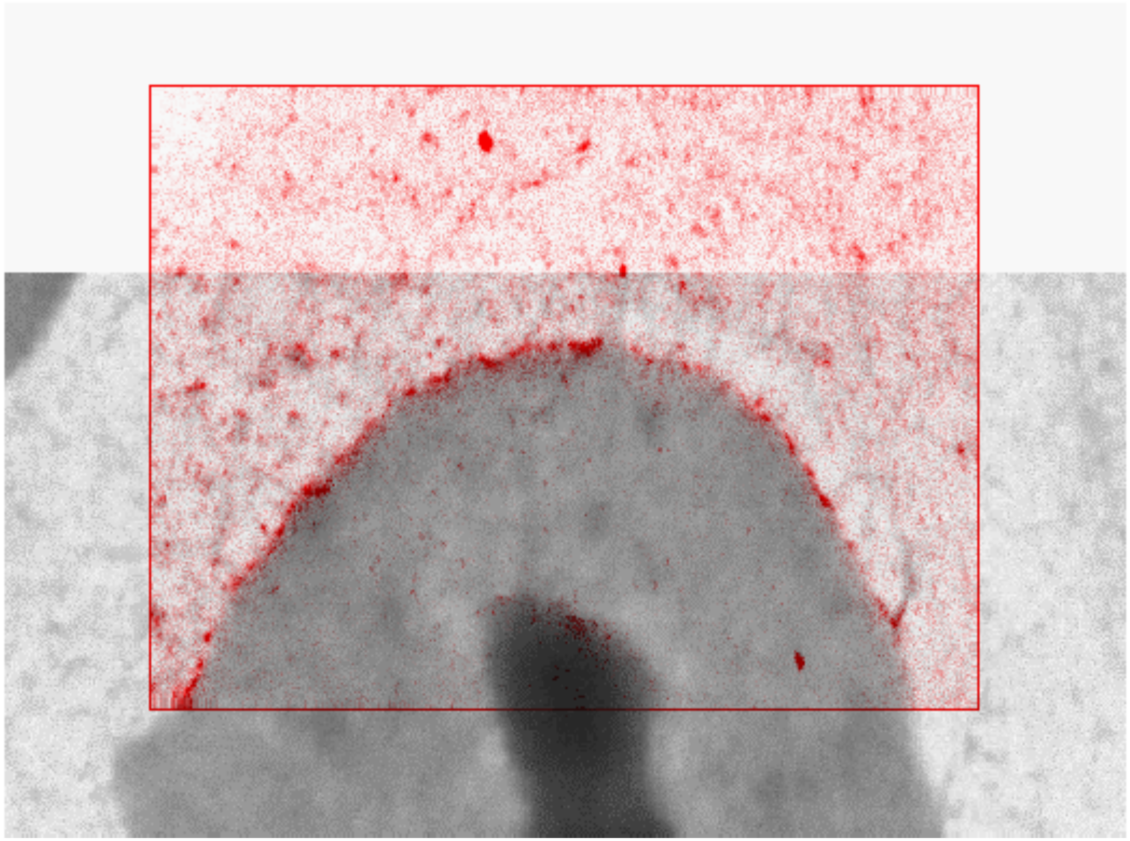

Brightfield image of a cell with Au labelling spheres overlayed with a darkfield image

Images acquired with STXM at the NSLS

S. Vogt, M.A. thesis, SUNY Stony Brook (1997).

Scanning X-ray microscope (STXM)

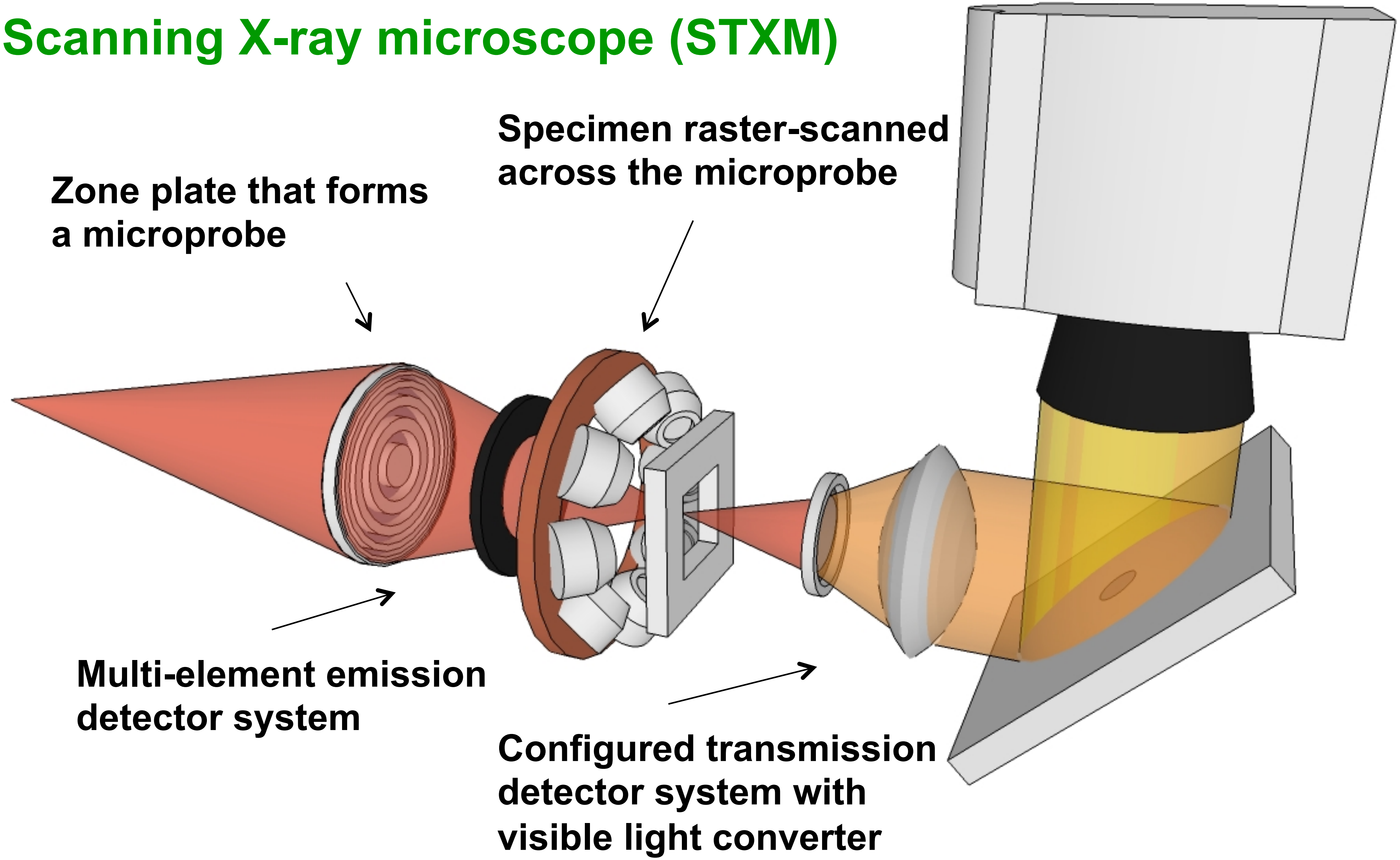

Detector based contrast technologies in scanning X-ray microscopy:

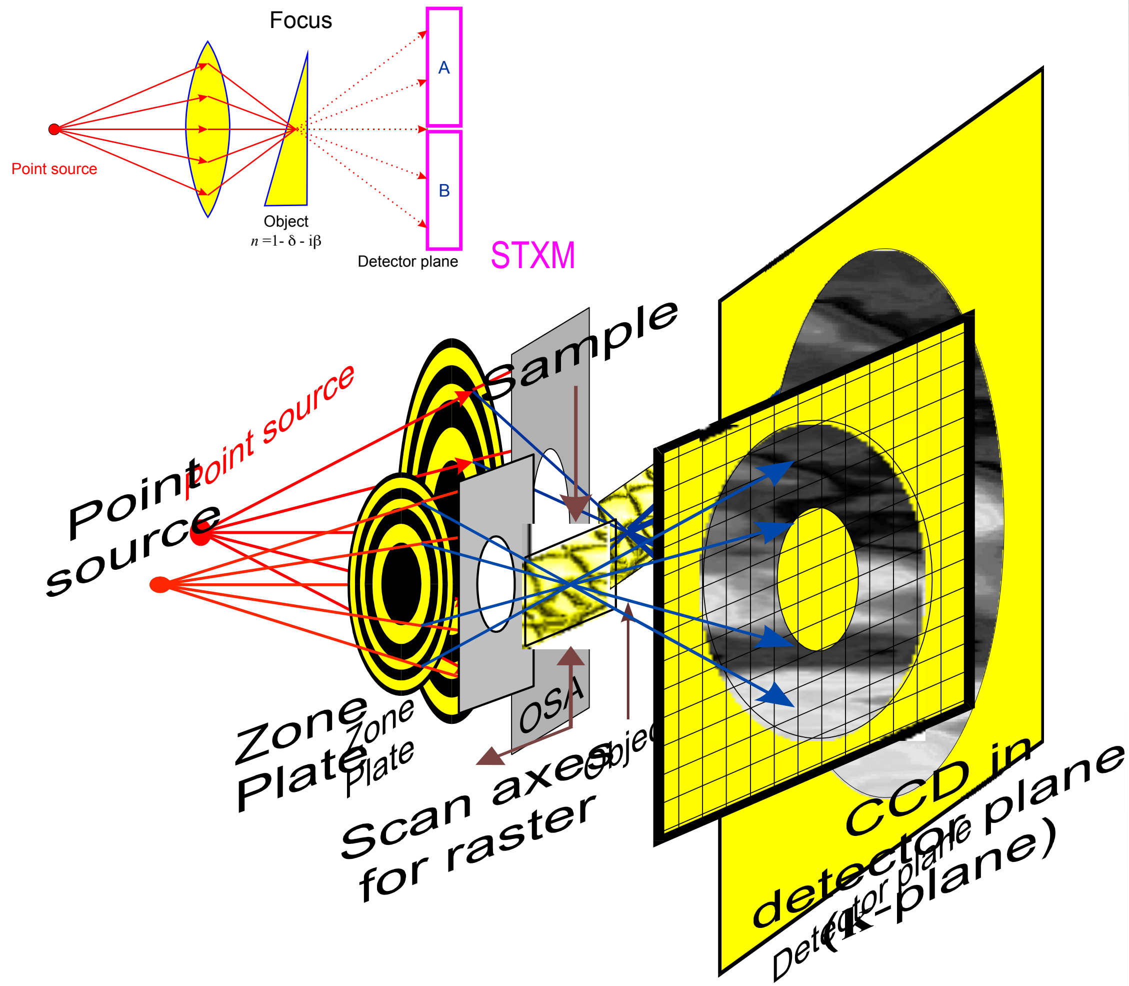

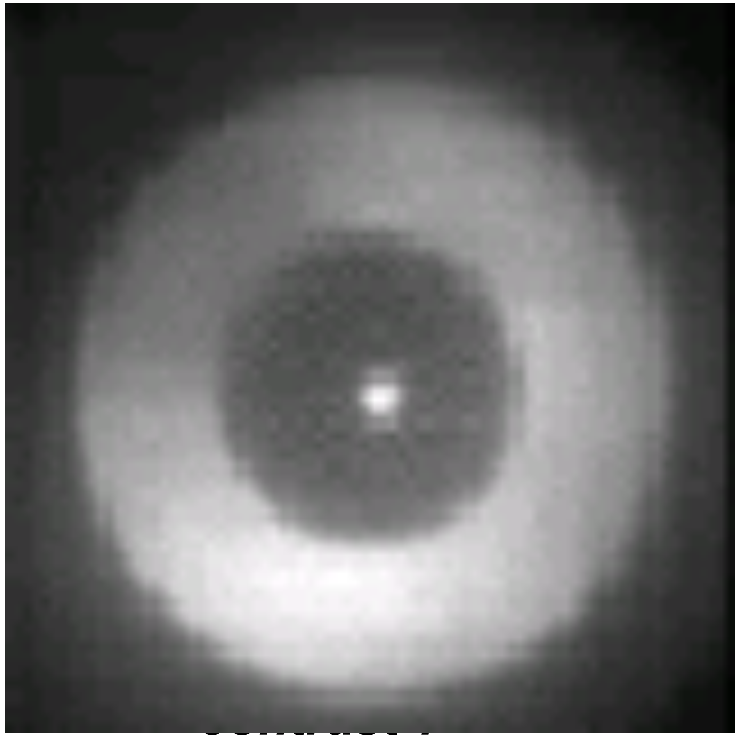

Acquired with Andor Ixon DV860A
Frame transfer back-illuminated Electron Multiplying CCD with shutter and light converting system (128x128px, 5 Mhz, 110f/s)

Scanning transmission mode

Differential phase contrast with a fast read-out CCD camera

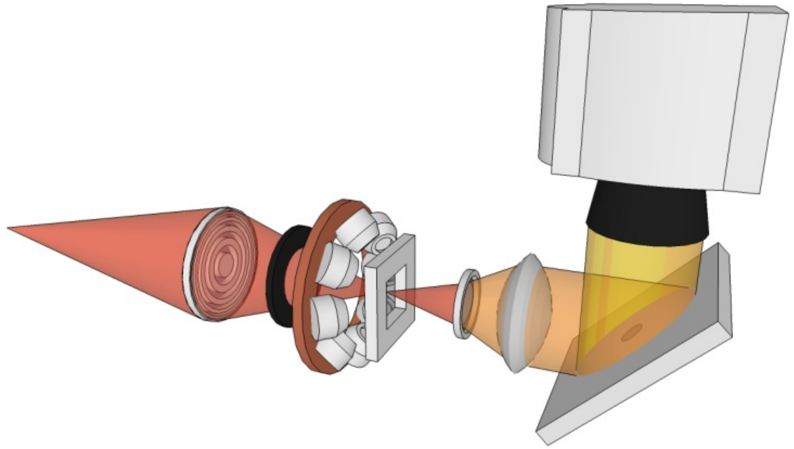

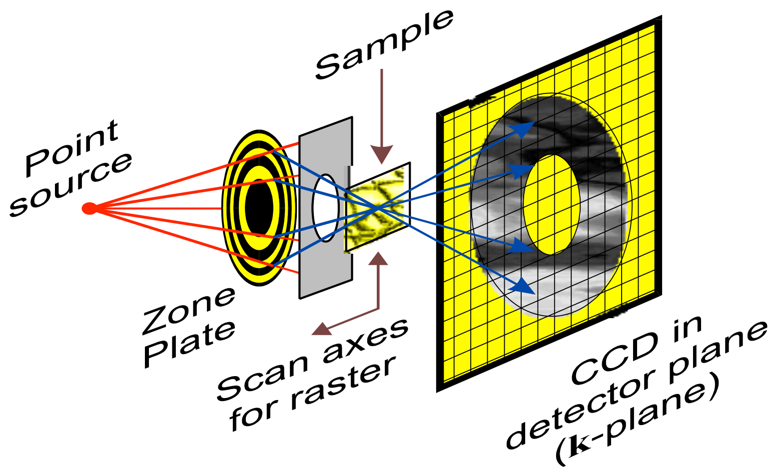

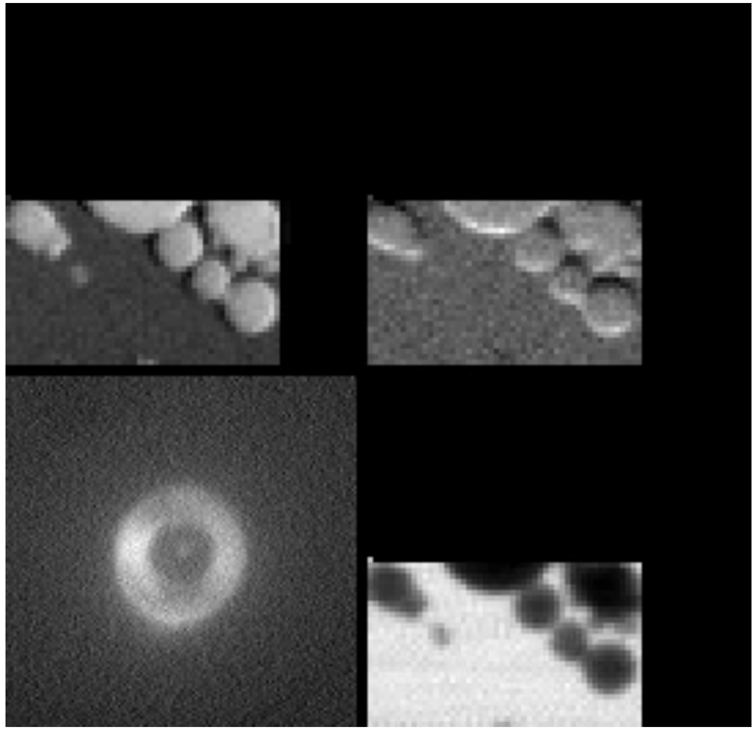

Simultaneous acquisition of:

- **Absorption or transmission**
- **Differential phase contrast**
- **Darkfield images**

Computational extraction of contrasts by masking:

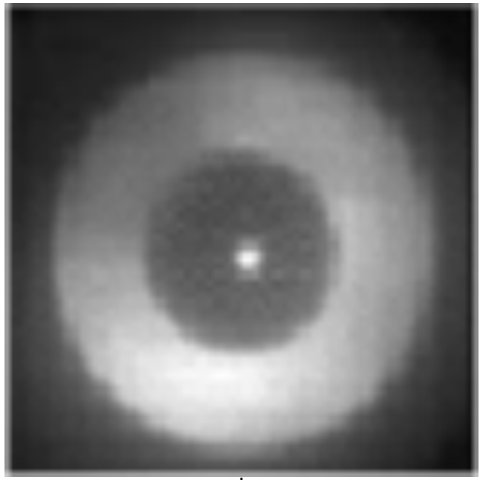

Raw data acquisition of first diffraction order image for each pixel of the raster scan

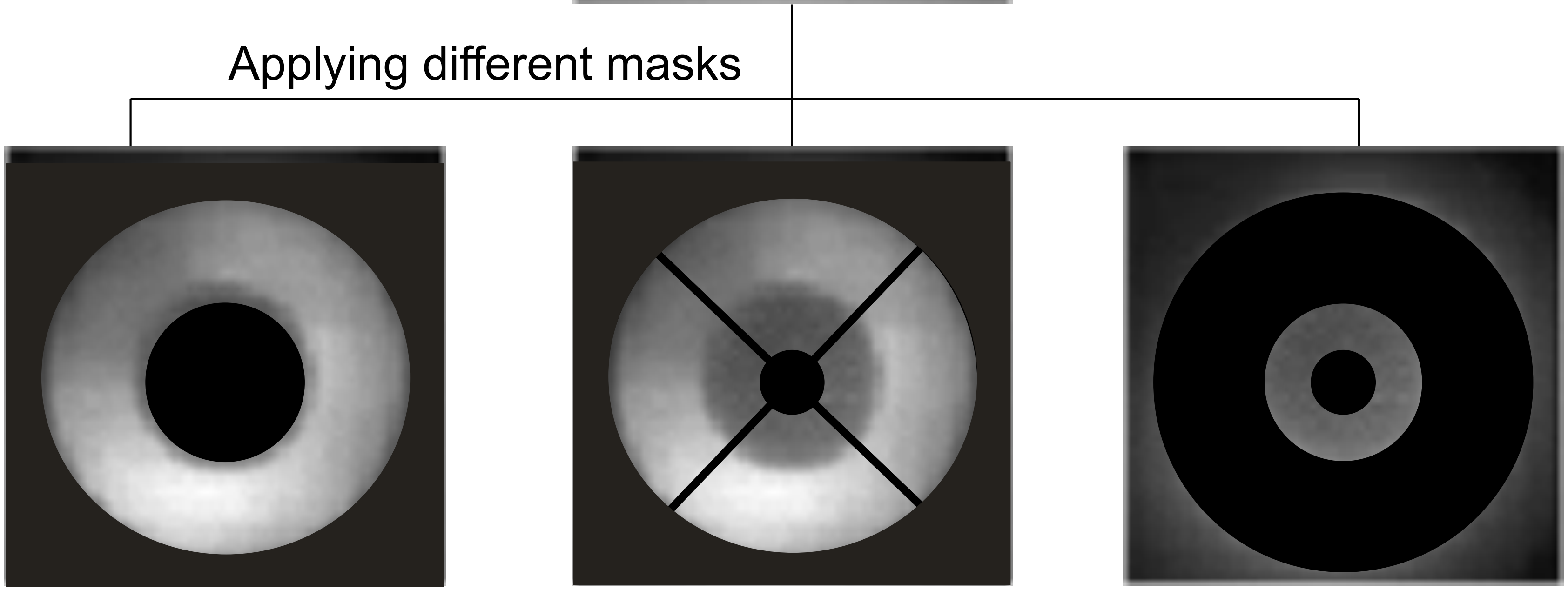

Bright field

Differential phase and absorption

Darkfield

A. Gianoncelli et al., Appl. Phys. Lett.

Principle: Differential phase contrast

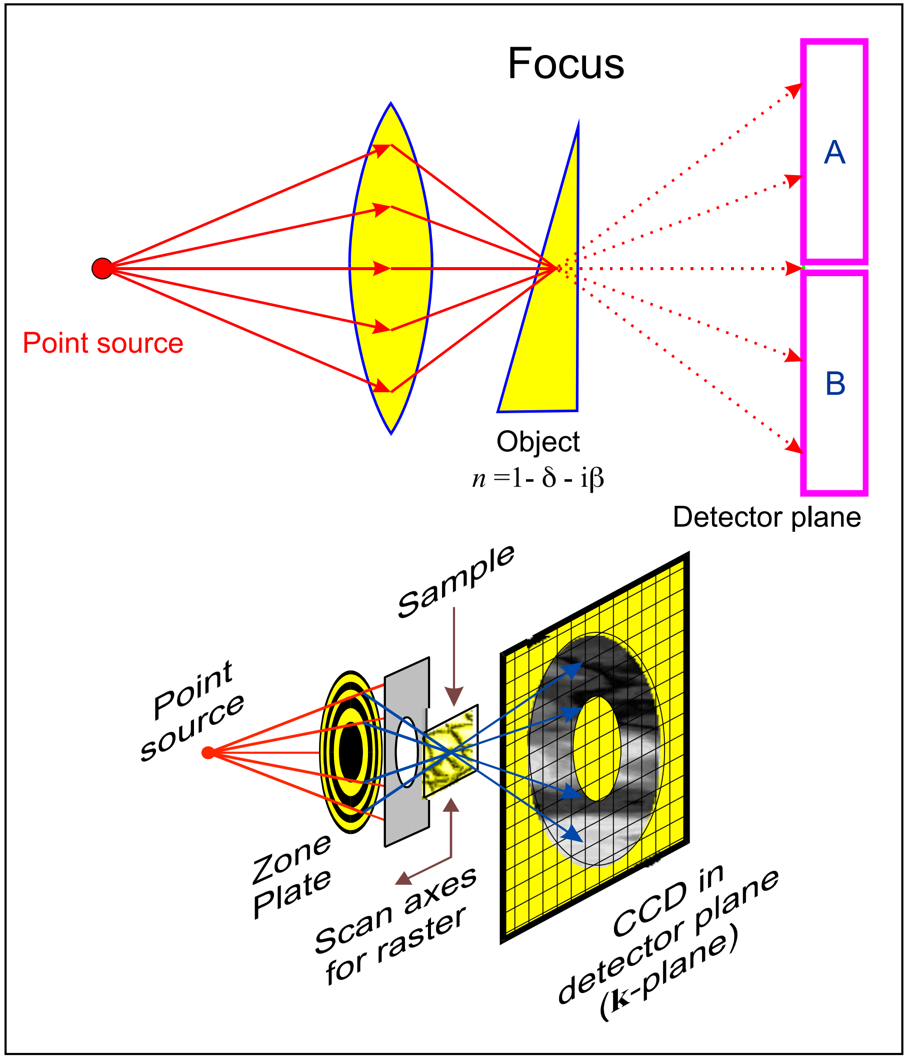

- The detector can be split into several elements
- The sum signal gives the incoherent bright-field signal
- Anti-symmetric signal combinations relate to the *phase gradient* of the object transmittance.

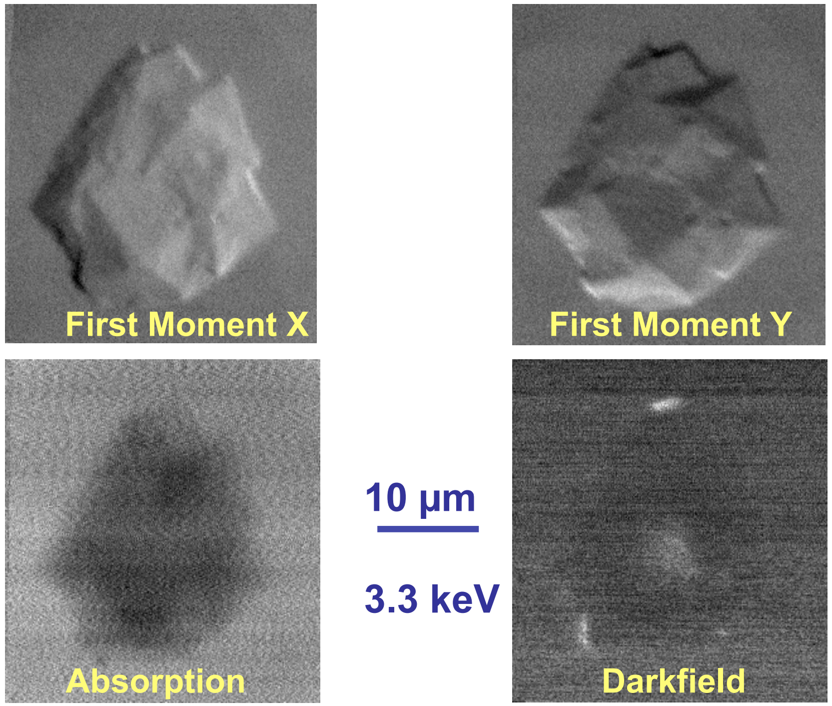

The benefit of a fast read-out, electron-multiplied CCD as configured detector in STXM

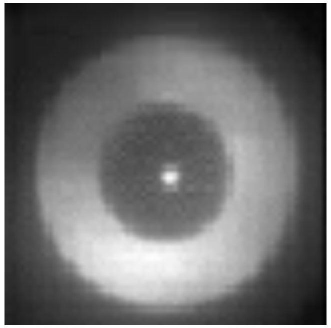

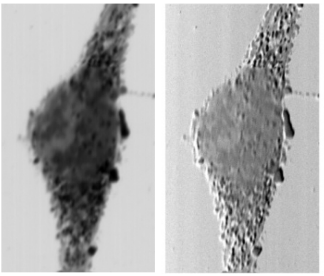

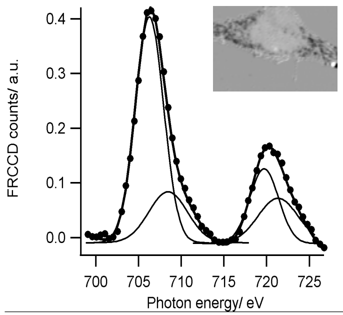

- Projection imaging for alignment purposes
- Simultaneous acquisition of absorption, differential phase contrast and darkfield imaging
- Diffraction imaging as ptychography
- XANES by across-edge imaging

Morrison, G. et al., IPAP Conf. Series 7, 377-379 (2006)
Gianoncelli A. et al., Appl Phys Lett 89, 251117 (2006)

G. R. Morrison,
A. Gianoncelli
King's College London

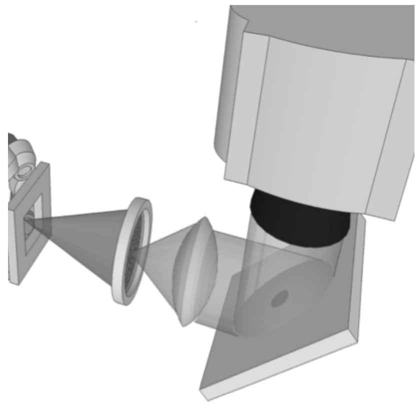

Marine biology: Imaging of giant diatoms

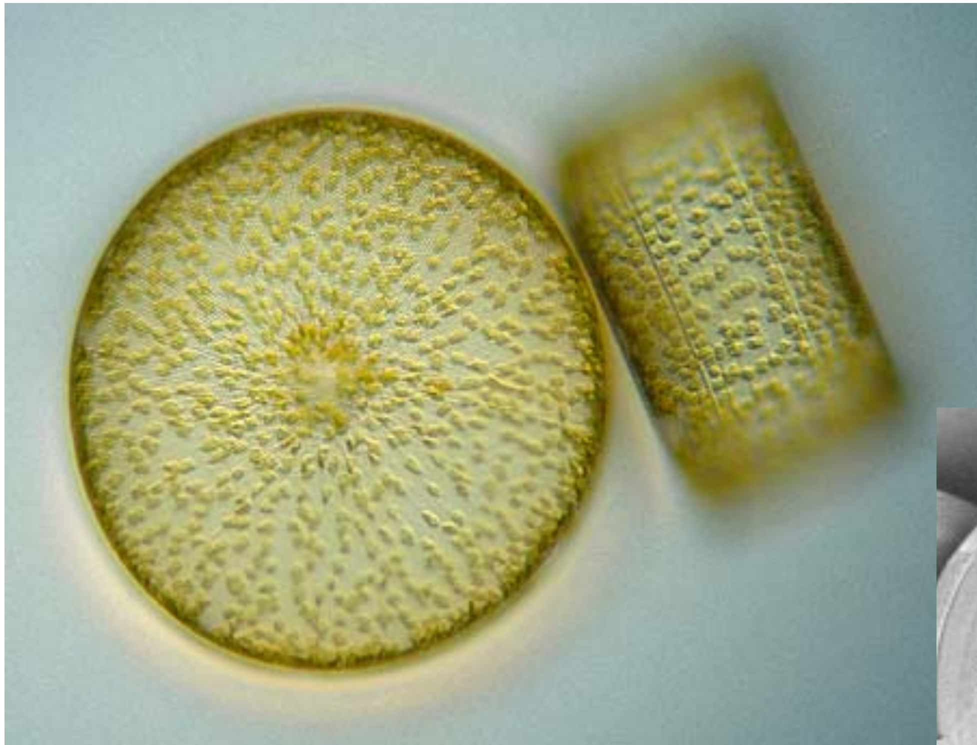

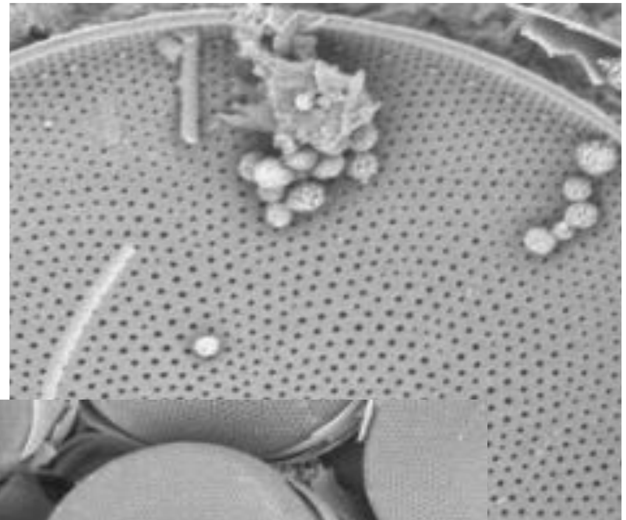

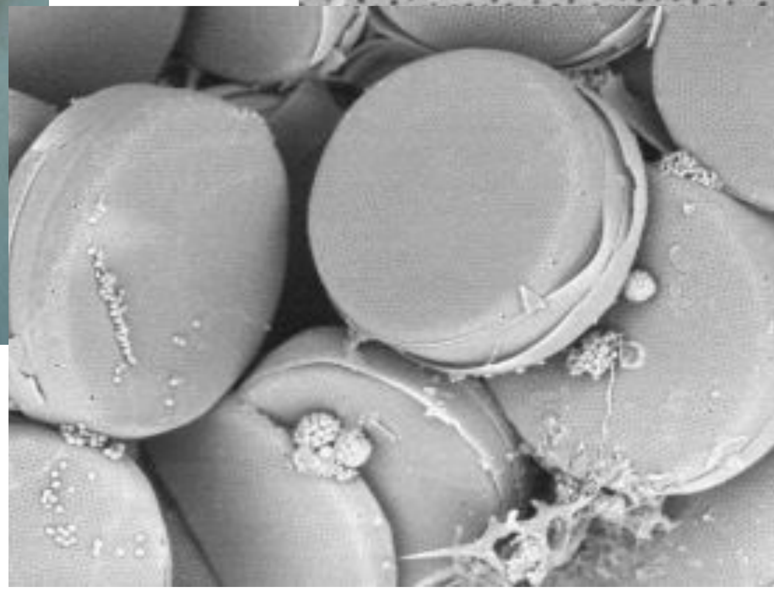

Planktonic diatom Coscinodiscus sp. (A. Beran, Laboratory for Marine Biology, Trieste, I)

Brightfield and differential phase contrast images acquired simultaneously with configured detector

Planktonic diatom "Casciodiscus sp." (provided by LBM, Trieste, I)

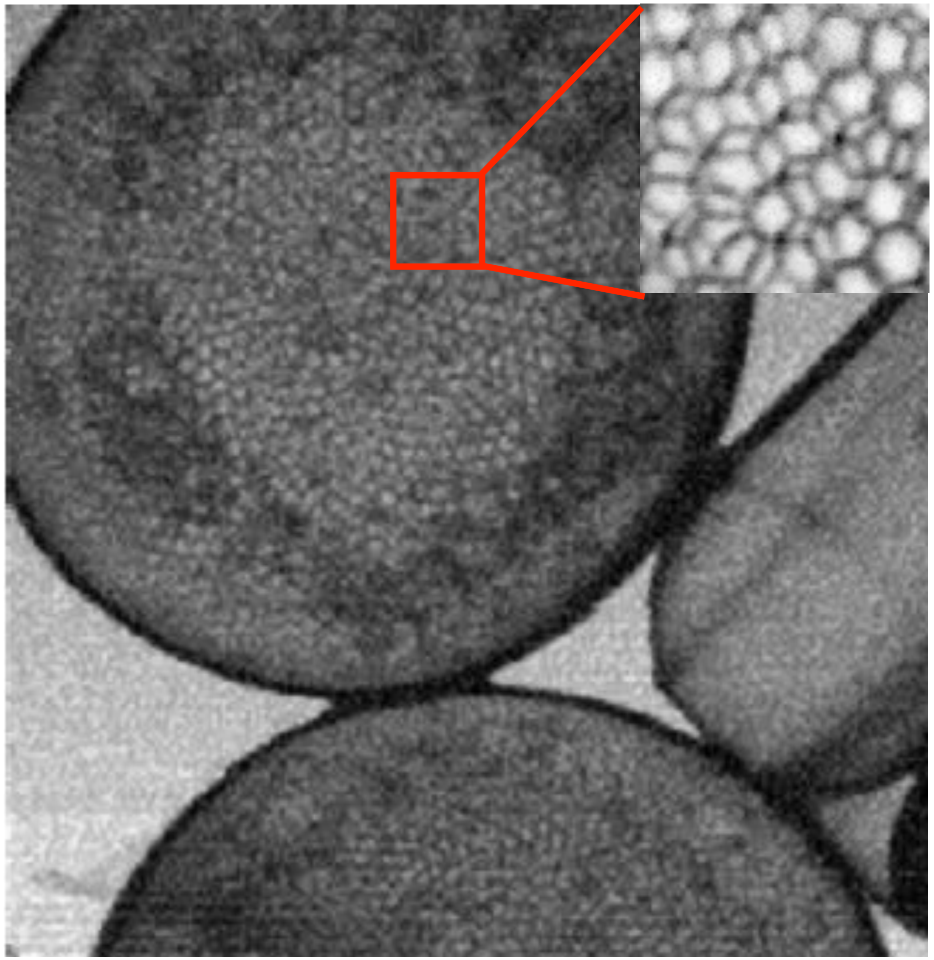

Bright field image

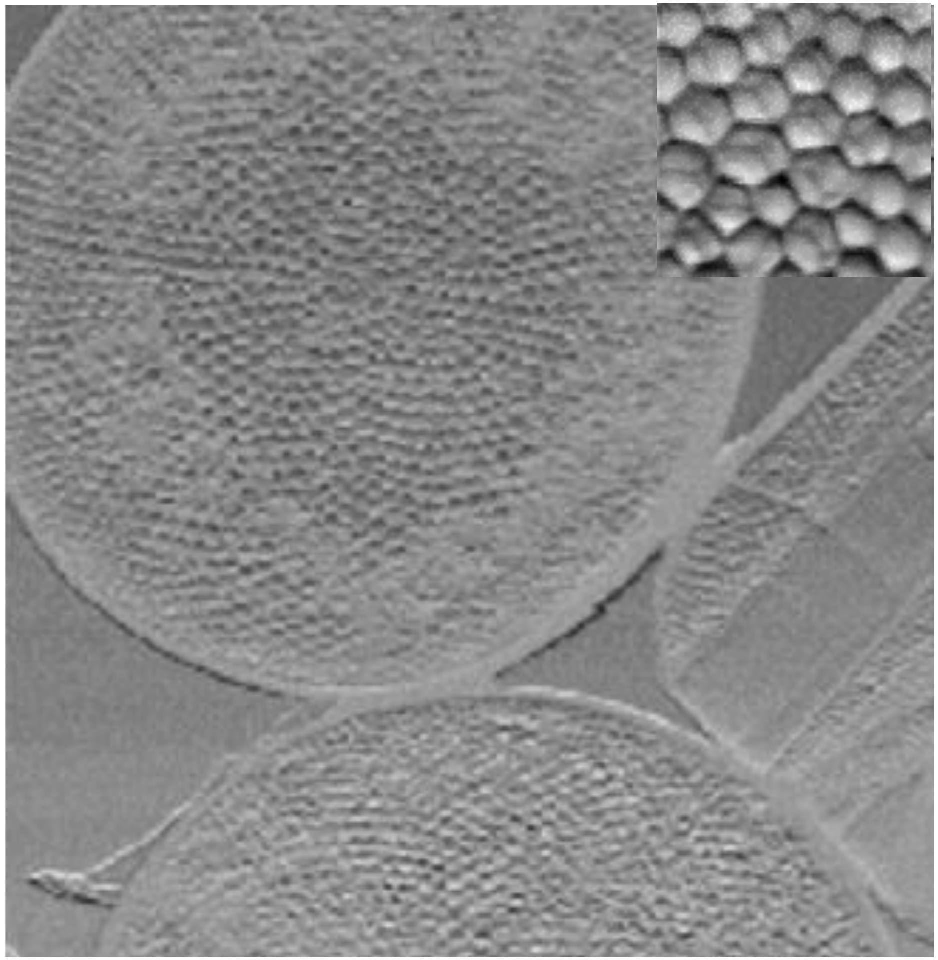

DPC mode – X-moment

Images acquired in STXM mode (TwinMic microscope) with FRCCD camera; E=1320 eV, 200x190 px, 50ms dwell/px

Brightfield and differential phase contrast images acquired simultaneously with configured detector




Coffee bean cell membranes

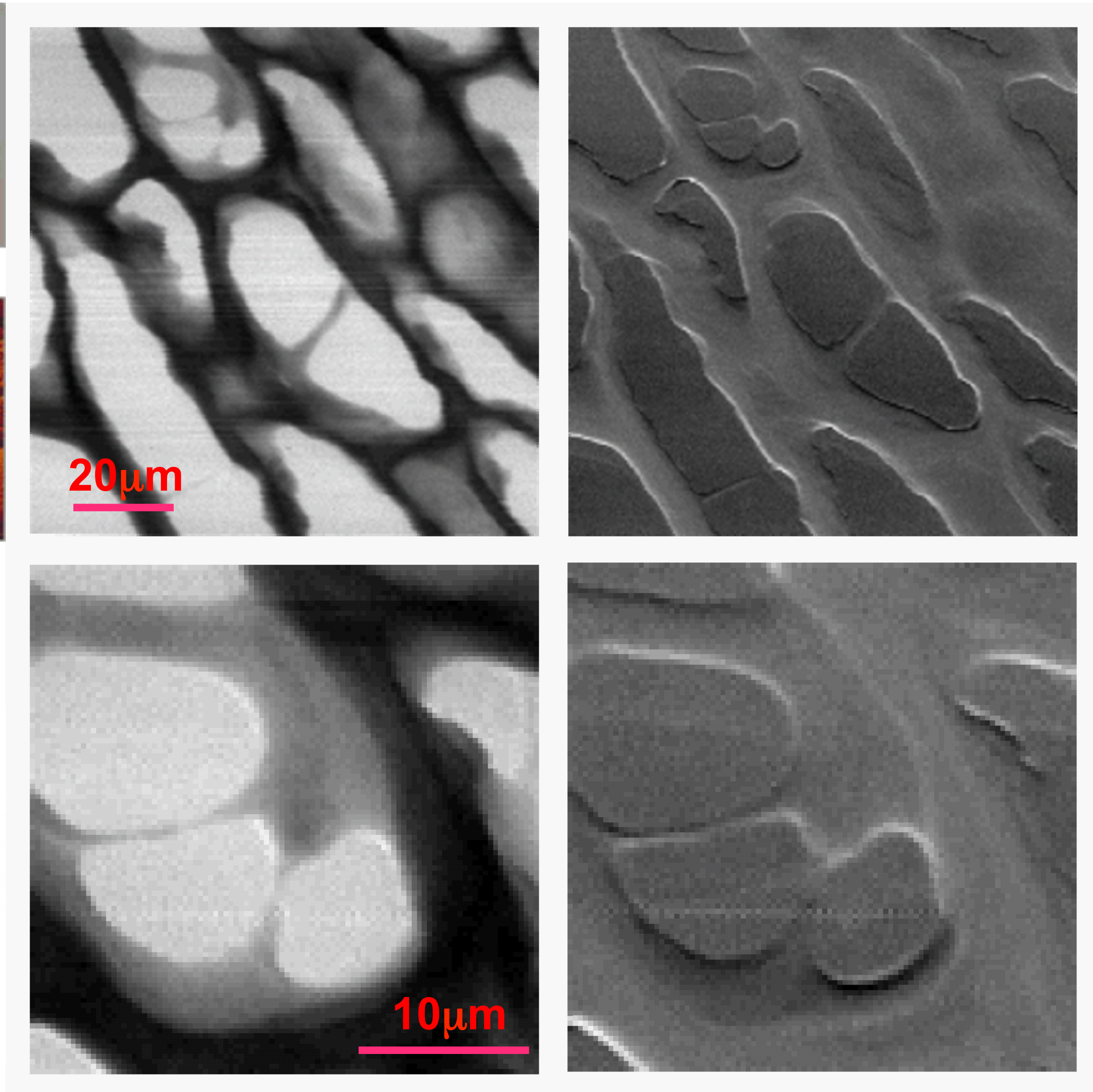

B. Bonnlaender, F. Sicilia, Illy AromaLab, et al.

Chemical/ Magnetic contrast

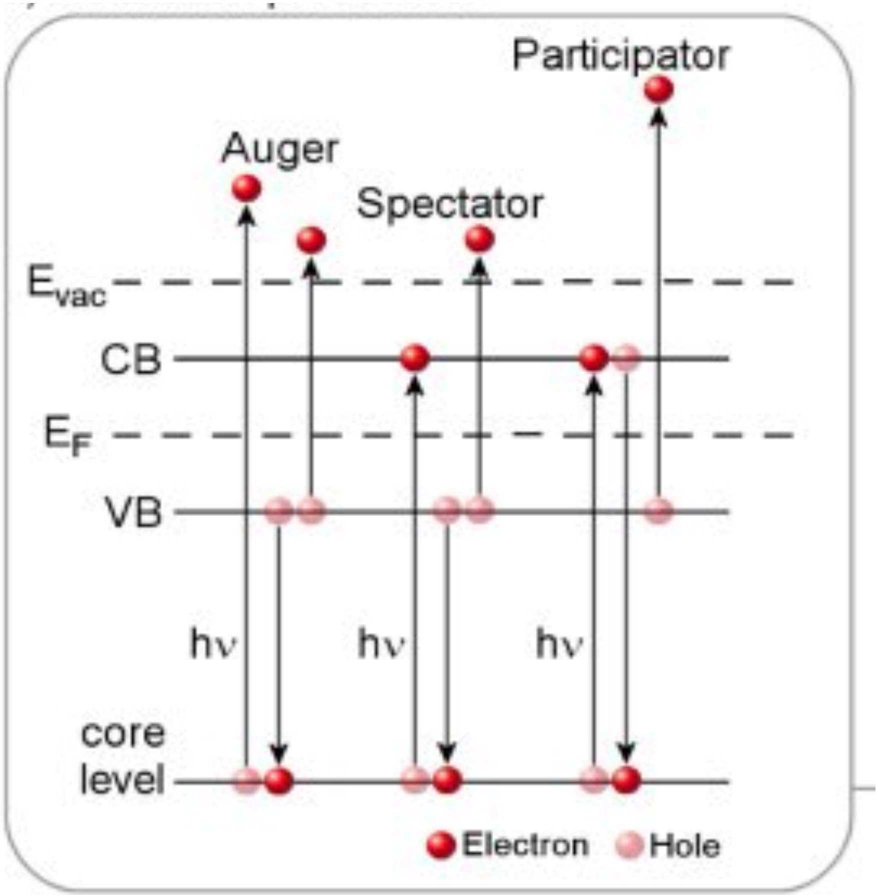

$$I \propto \exp(-\mu d) \quad , \quad \mu \propto \frac{Z^z}{(h\nu)^3}$$

XANES = X-ray Absorption Near Edge Spectroscopy

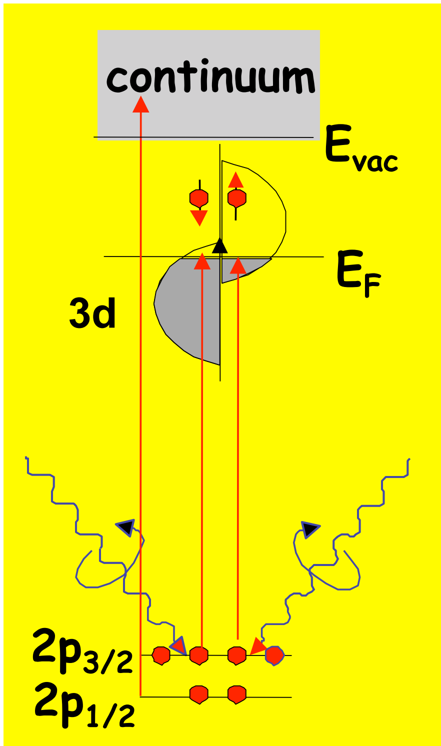

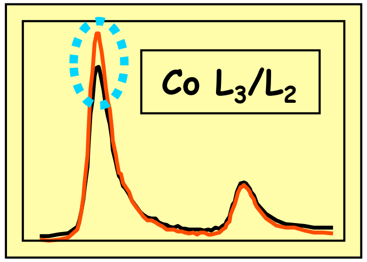

Resonances with unfilled states.

XANES: tuning on molecular orbitals
XMLD: imaging antiferromagnets,
XMCD: imaging ferromagnets

Chemical contrast

Outlining the lateral distribution of PS/ PMMA

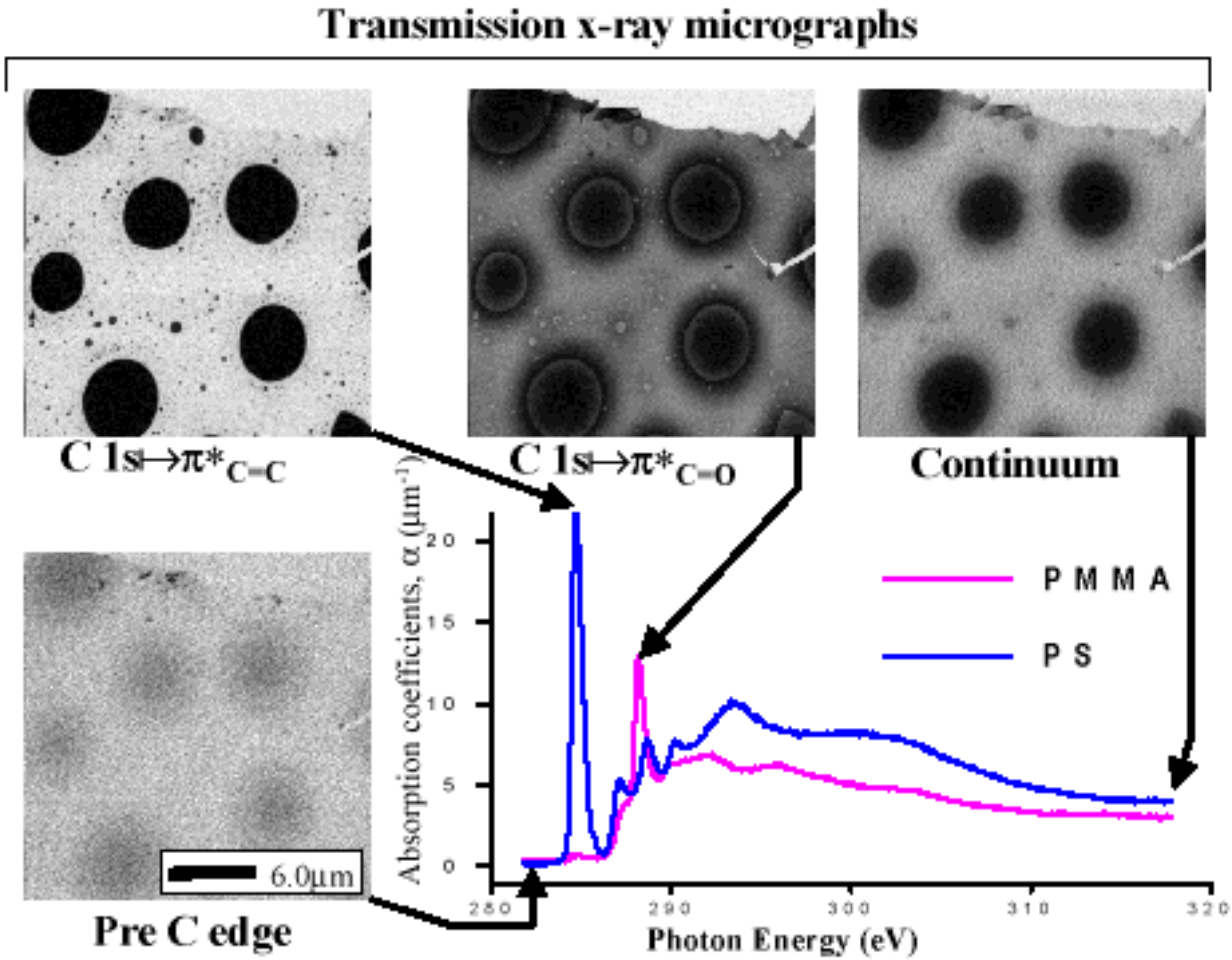

H. Ade, SUNY-SB STXM at the NSLS

Photoionization

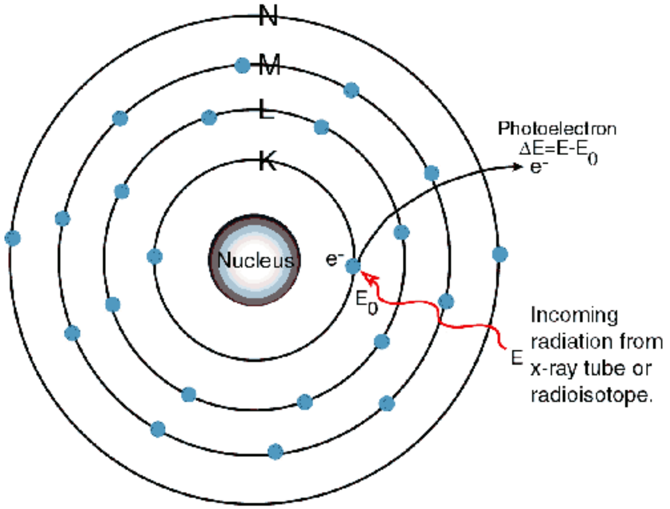

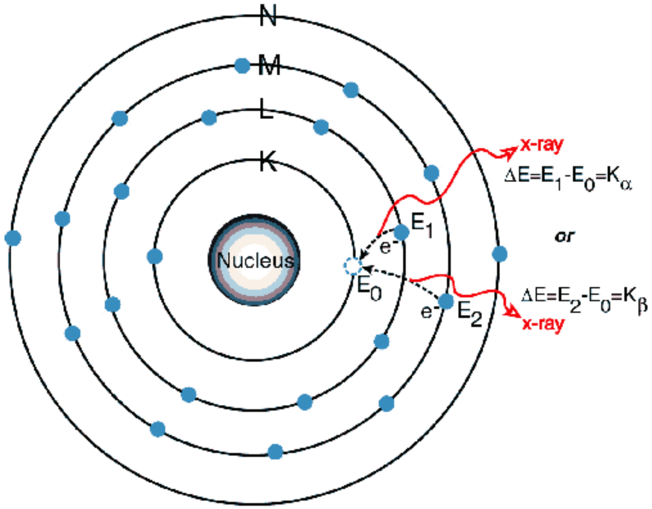

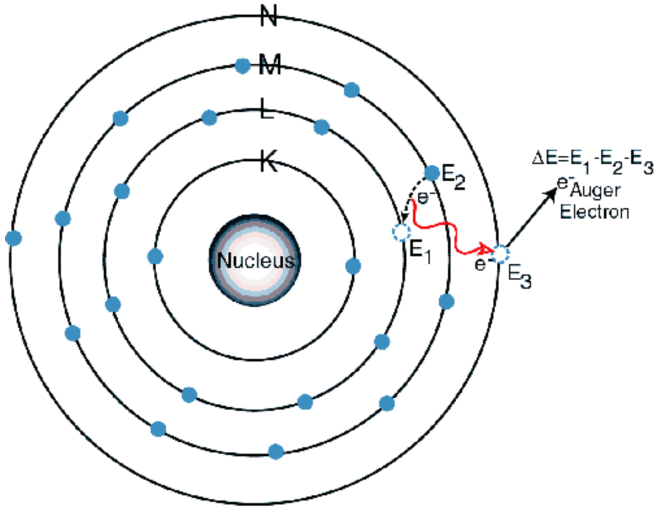

X-ray absorption

(through photoelectric effect)

The primary X-ray photon causes the ejection of electrons from the inner shells, creating vacancies

X-ray Fluorescence

The vacancy created by the primary X-ray photon is filled by an electron coming from an outer shell causing the emission of a characteristic X-ray photon whose energy is the difference between the two binding energies of the corresponding shells

Auger effect

The vacancy created by the primary X-ray photon is filled by an electron coming from an outer shell and the energy is transferred directly to one of the outer electrons, causing it to be ejected from the atom.

Chemical sensitivity of X-rays: Elemental mapping

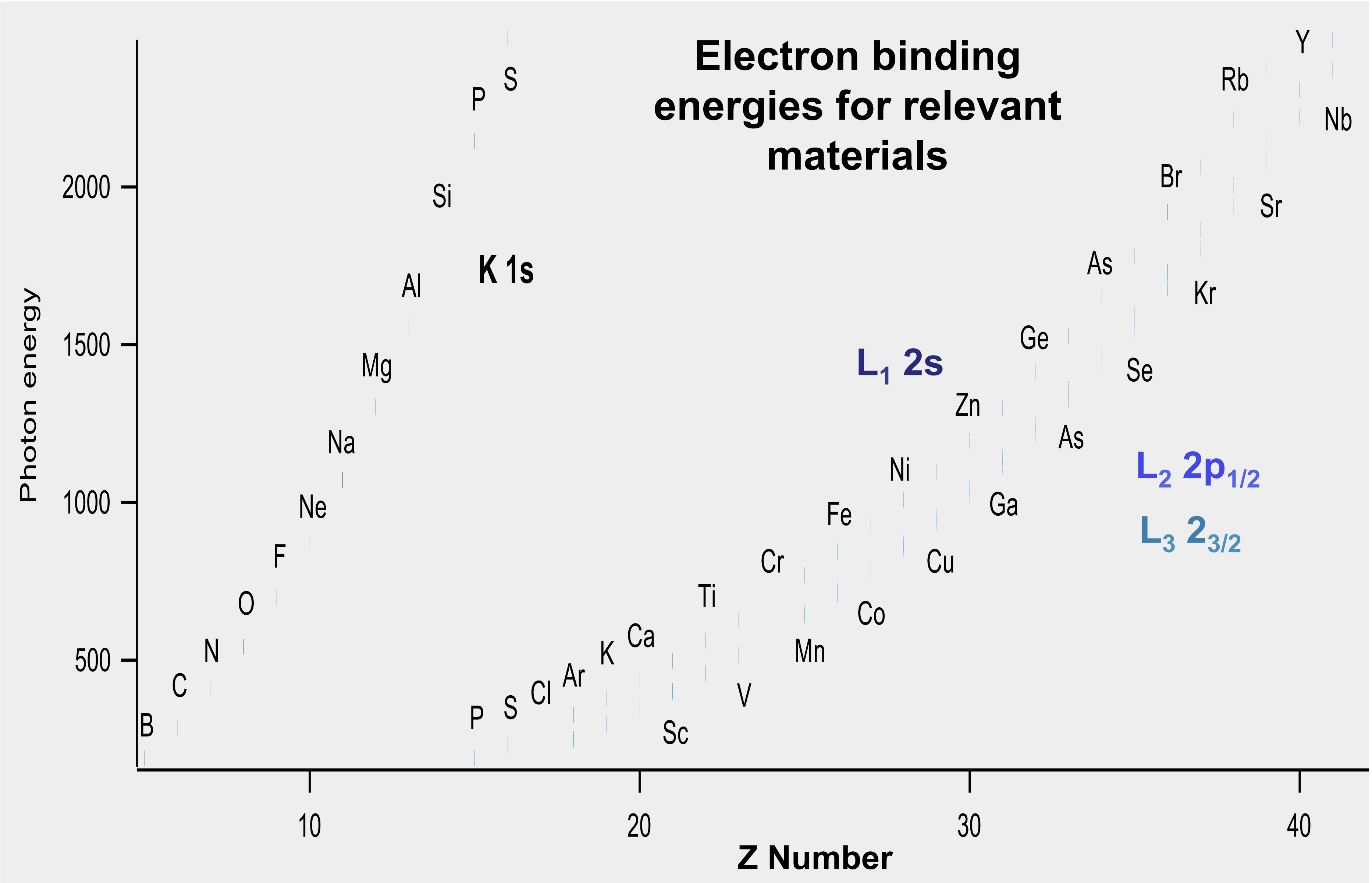

Fluorescence contrast

- Microprobe focused on the sample
- Sample raster scanned
- Analysis of each spectrum in the raster scan
- Construction of an X,Y map for each chemical elements present in the spectrum

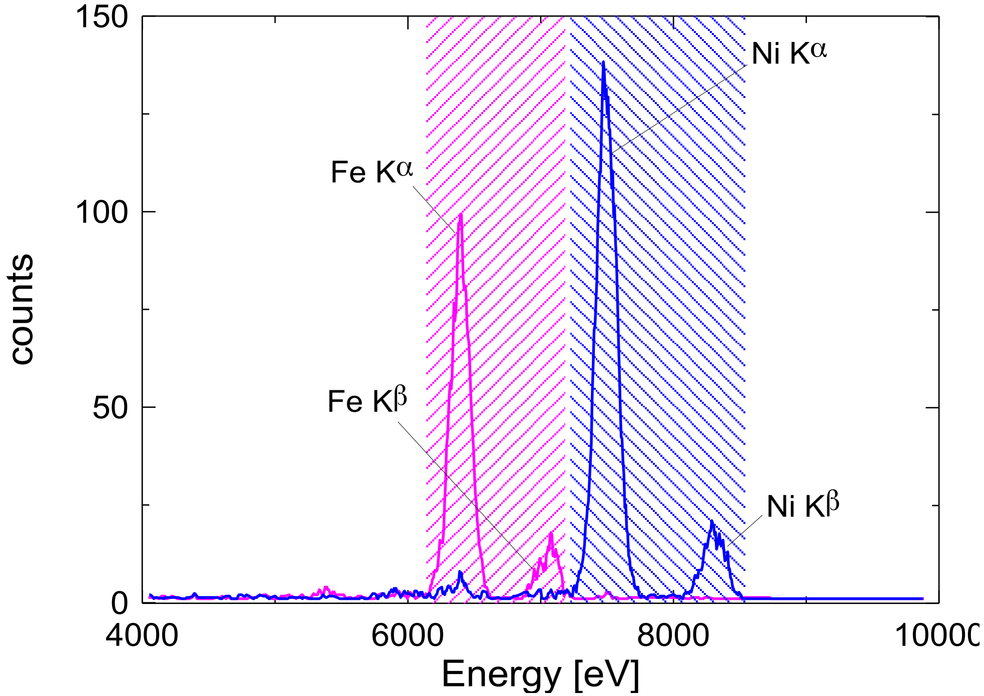

Low-energy X-ray fluorescence for elemental analysis:

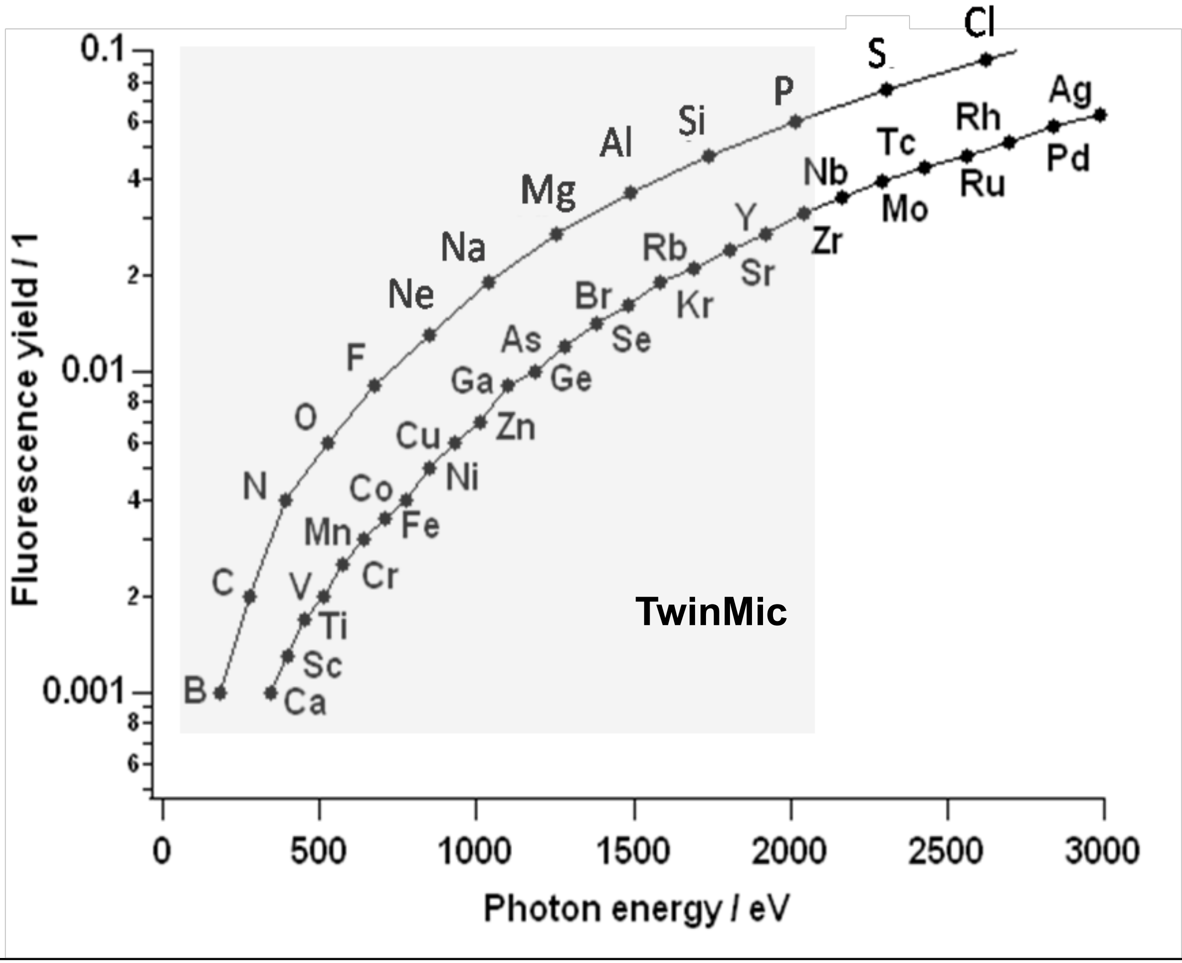

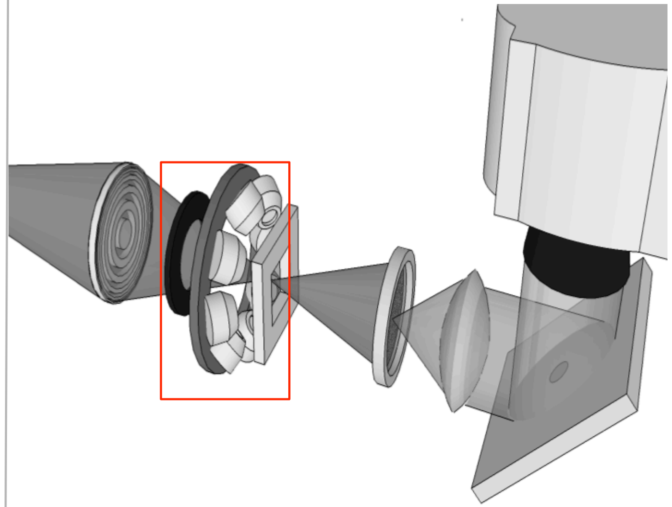

Detecting trace elements:

X-ray fluorescence:
~1000x better sensitivity than electrons for trace elemental mapping (ion concentrations etc.).

Low fluorescence yields for soft X-rays! !!

A. Gianoncelli, B. Kaulich, M. Kiskinova, R. Alberti, T. Klatka, A. Longoni, A. de Marco, A. Marcello, Simultaneous Soft X-ray Transmission and Emission Microscopy, Nucl. Instr. and Meth. A 608 (1), 195-198

Low-energy X-ray fluorescence

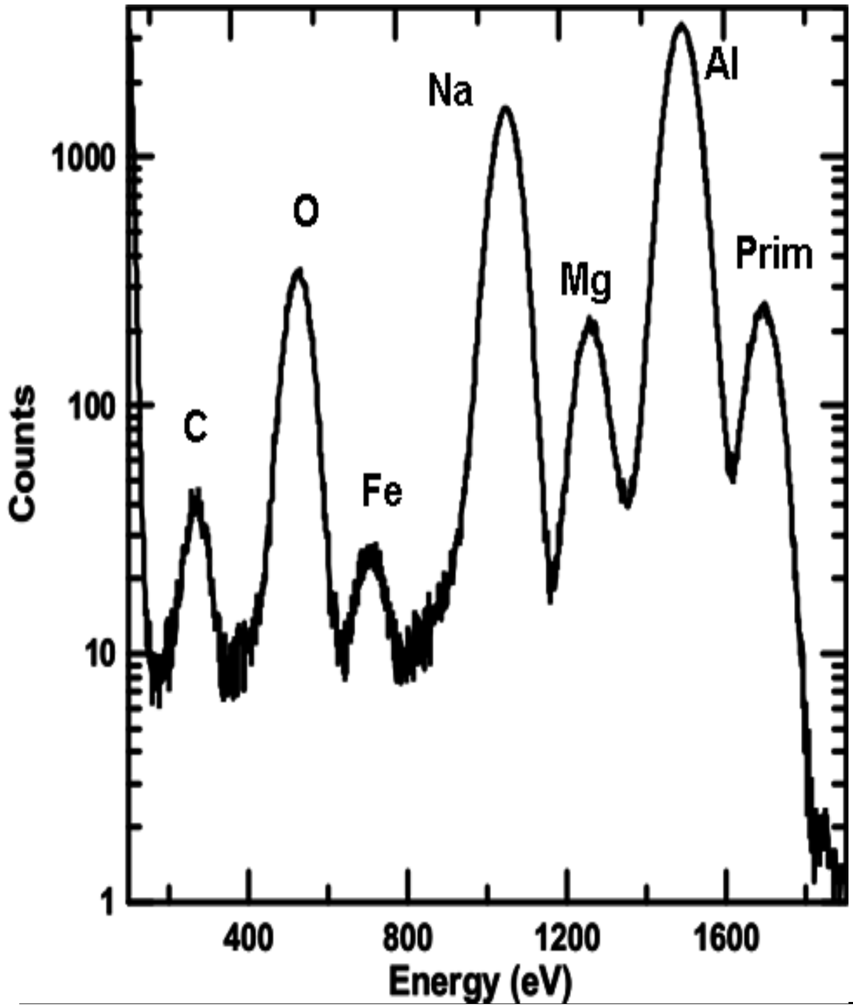

TwinMic LEXRF spectrum with unfocused beam of a test organic matrix on a metal shim

Dynamic range: up to 30 kcounts/s

Average FWHM energy resolution @ C- K edge: 69 eV

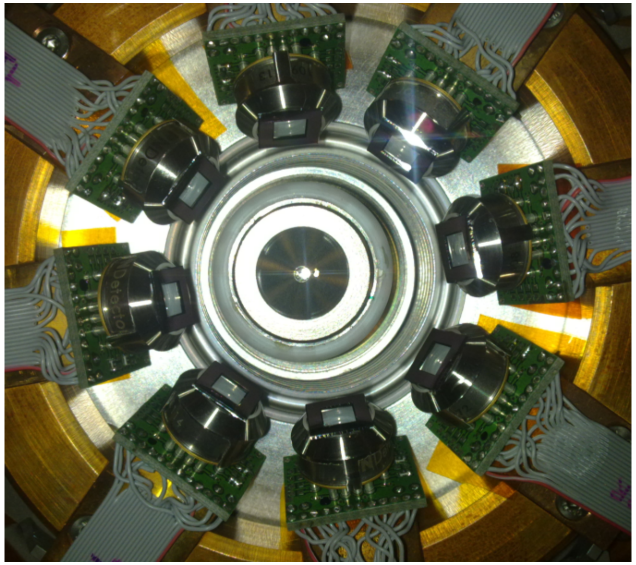

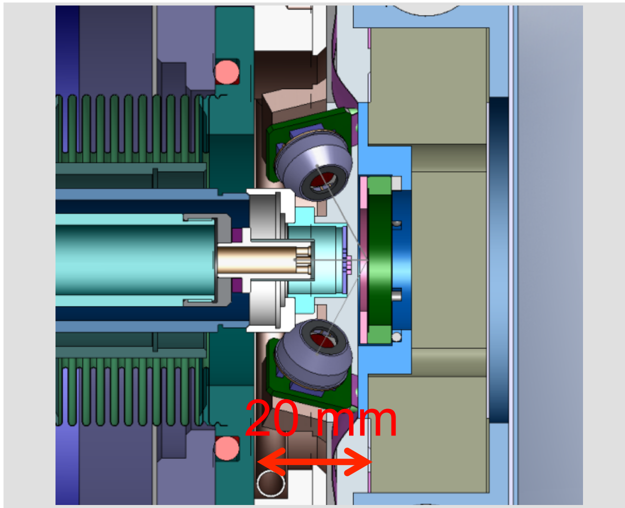

A. Gianoncelli, B. Kaulich, M. Kiskinova, R. Alberti, T. Klatka, A. Longoni, A. de Marco, A. Marcello, Simultaneous Soft X-ray Transmission and Emission Microscopy, Nucl. Instr. and Meth. A 608 (1), 195-198

Food Science: Inside the wheat

Ivan Kreft,
University Ljubljana

Functionality and toxicity of Zn in wheat and buckwheat analyzed on sub-cellular level

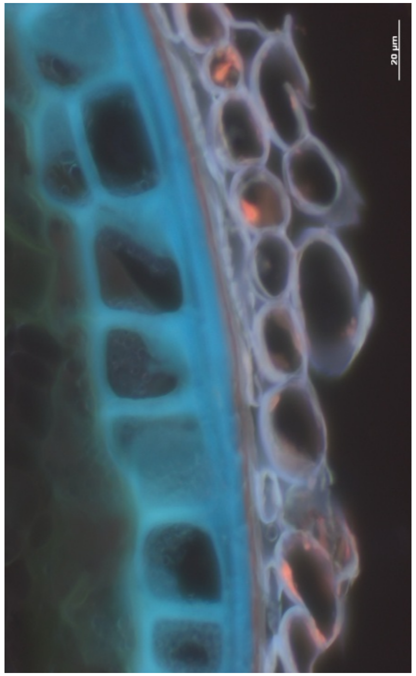

Structure of a wheat grain

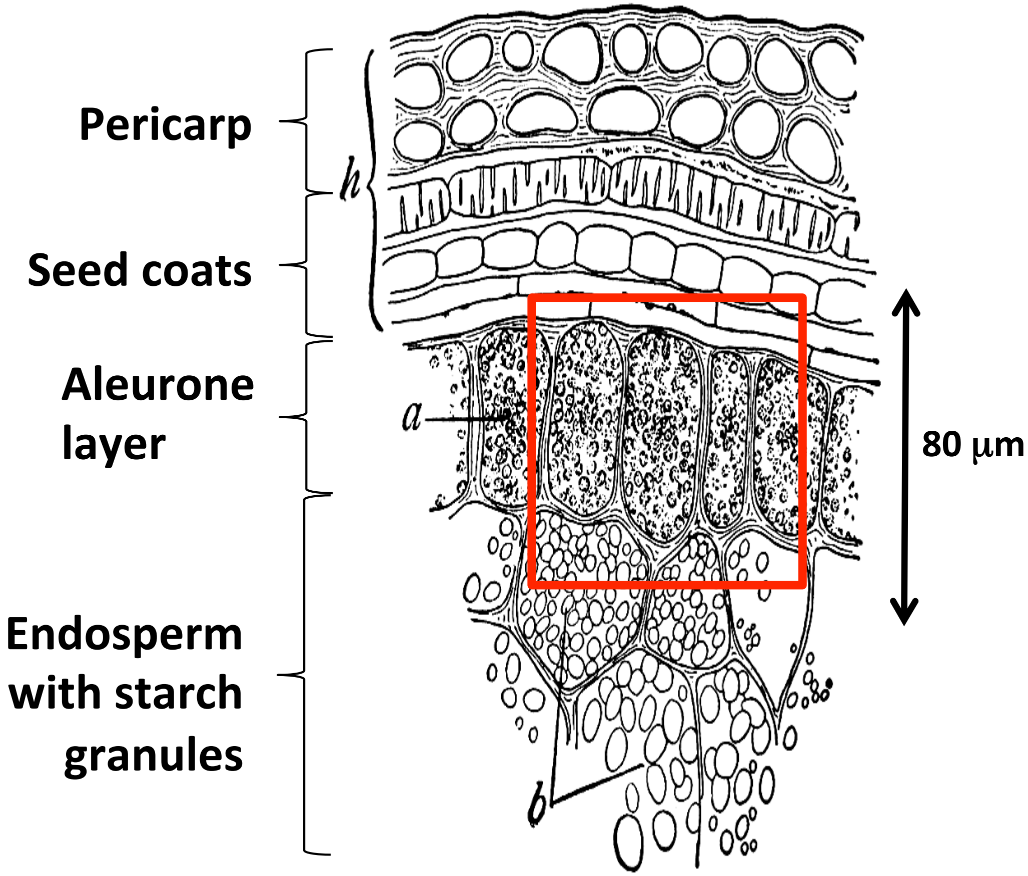

M. Regvar, D. Eichert, B. Kaulich, A. Gianoncelli, P. Pongrac, K. Vogel-Mikus, I. Kreft, New insights into globoids of protein storage vacuoles in wheat aleurone using synchrotron soft X-ray microscopy, Journal of Experimental Botany, Vol. 62, No. 11, 3929–3939, 2011.

Ivan Kreft,
Fac. of Biotechnology,
University Ljubljana

Functionality and toxicity of Zn in wheat and buckwheat analyzed on sub-cellular level

Healthy control wheat

E=1686 eV
80 x 80 mm^2
80 x 80 px
8 s dwell/ px
1 mm resolution
4 detectors

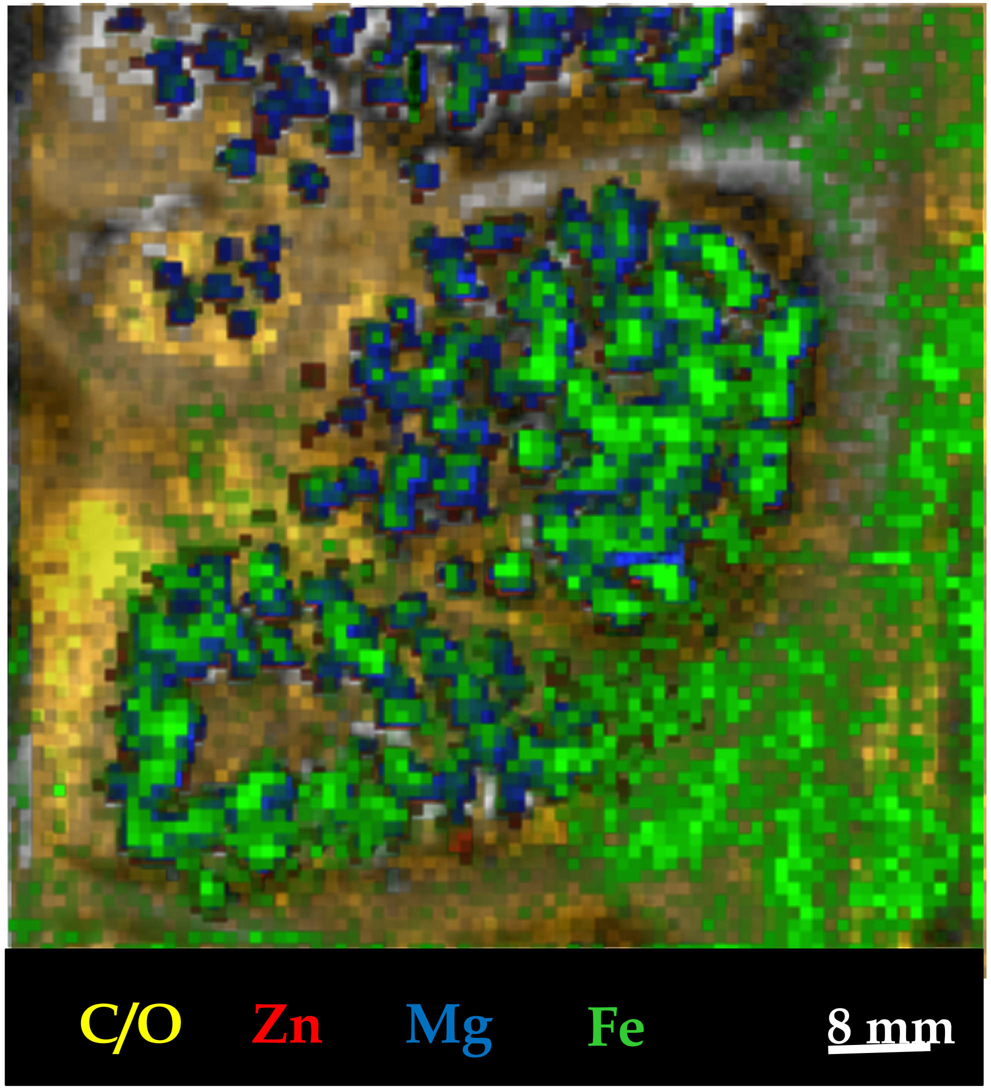

M. Regvar, D. Eichert, B. Kaulich, A. Gianoncelli, P. Pongrac, K. Vogel-Mikus, I. Kreft, New insights into globoids of protein storage vacuoles in wheat aleurone using synchrotron soft X-ray microscopy, Journal of Experimental Botany, Vol. 62, No. 11, 3929–3939, 2011.

Ivan Kreft,
Fac. of Biotechnology,
University Ljubljana

Functionality and toxicity of Zn in wheat and buckwheat analyzed on sub-cellular level

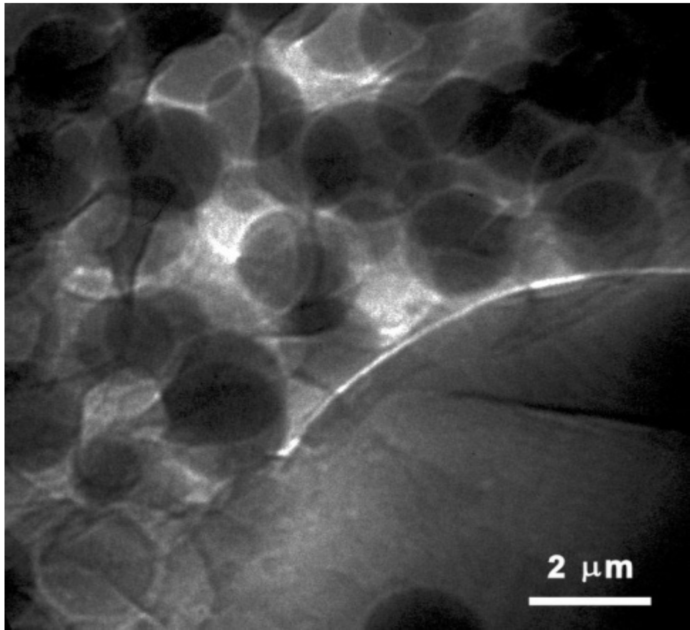

TXM images acquired with a double-frequency ZP (15nm outermost zone width from J. Vila-Comamala (PSI)

1s dwell, 740 eV photon energy

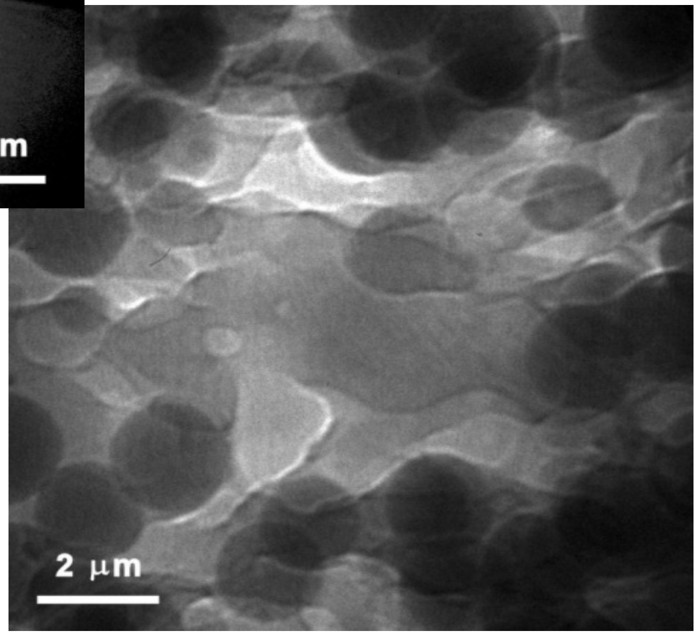

M. Regvar, D. Eichert, B. Kaulich, A. Gianoncelli, P. Pongrac, K. Vogel-Mikus, I. Kreft, New insights into globoids of protein storage vacuoles in wheat aleurone using synchrotron soft X-ray microscopy, Journal of Experimental Botany, Vol. 62, No. 11, 3929–3939, 2011.

Nanotoxicology: $CoFe_2O_4$ ENPs

G. Ceccone,
P. Marmorato et al.,
EC Joint Research Center, Ispra, I

Localization of engineered nanoparticles (ENPs) inside a cell and on the possible effects on the cell metabolic behaviour

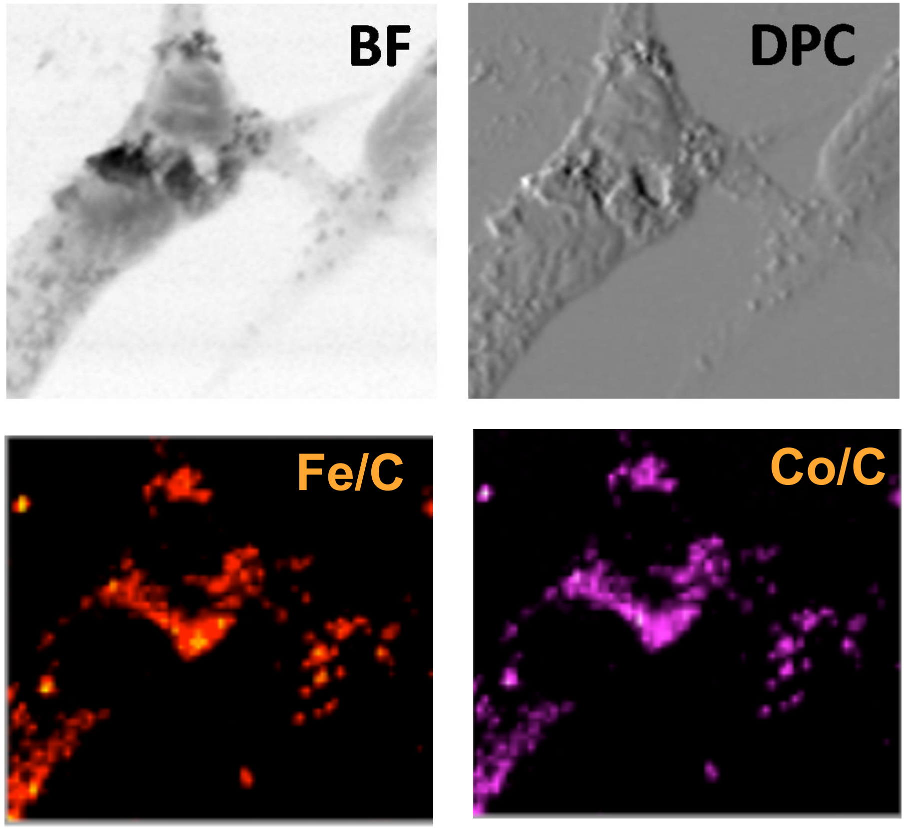

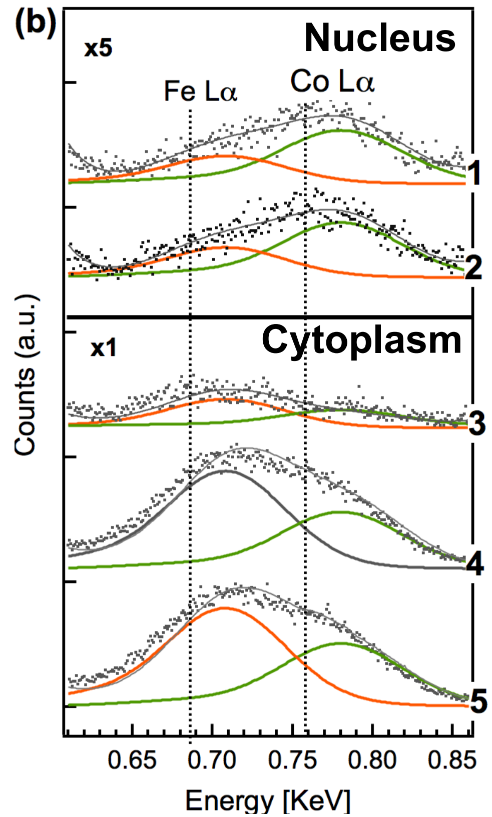

$CoFe_2O_4$ in mouse 3T3 fibroblast cells, E=2019 eV, 60um x 60 um, 80 x 80 pixels, 15s/pixel

P. Marmorato, G. Ceccone, A. Gianoncelli, L. Pascolo, J. Ponti, F. Rossi, M. Salomé, B. Kaulich, and M. Kiskinova, Cellular distribution and degradation of Cobalt Ferrite Nanoparticles in Balb/3T3 Fibroblasts, in press in Toxicology Letters

Nanotoxicology: $CoFe_2O_4$ ENPs

Control

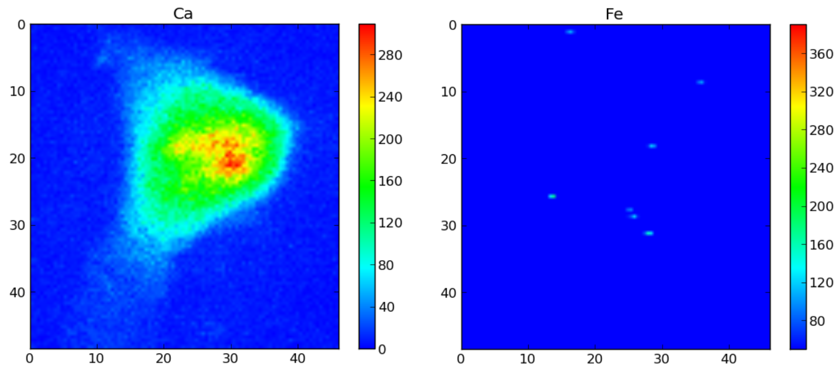

Exposed to 500μM

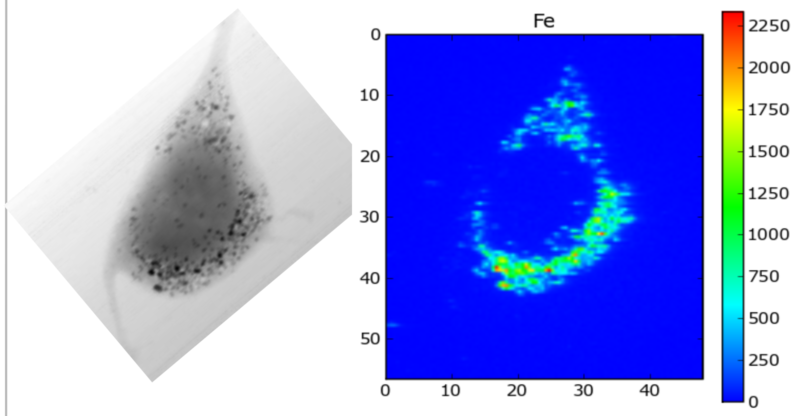

Exposed to 40μM

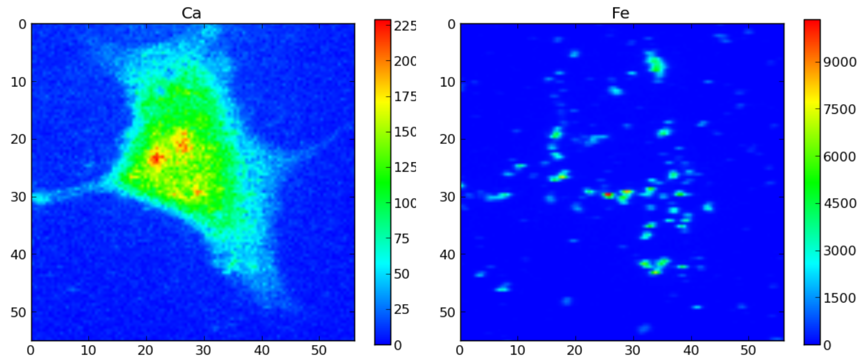

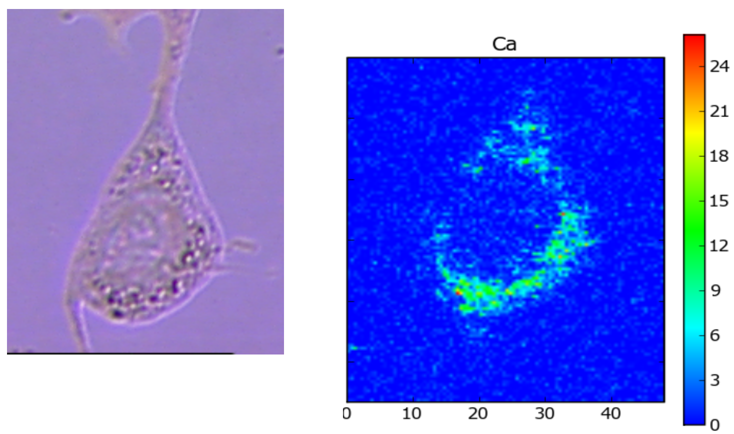

P. Marmorato, G. Ceccone, A. Gianoncelli, L. Pascolo, J. Ponti, F. Rossi, M. Salomé, B. Kaulich, and M. Kiskinova, Cellular distribution and degradation of Cobalt Ferrite Nanoparticles in Balb/3T3 Fibroblasts, Toxicology Letters 2 (2011) 128-136.

Clinical medicine: Asbestos in lung tissue

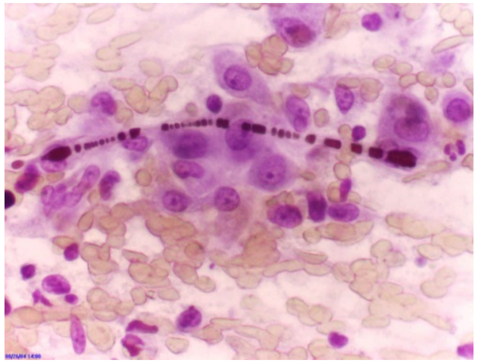

M. Melato,
Monfalcone Hospital
L. Pascolo,
Sincrotrone Trieste

Mesothelioma and differentiation of lung tissue due to asbestos;
the role of Mg

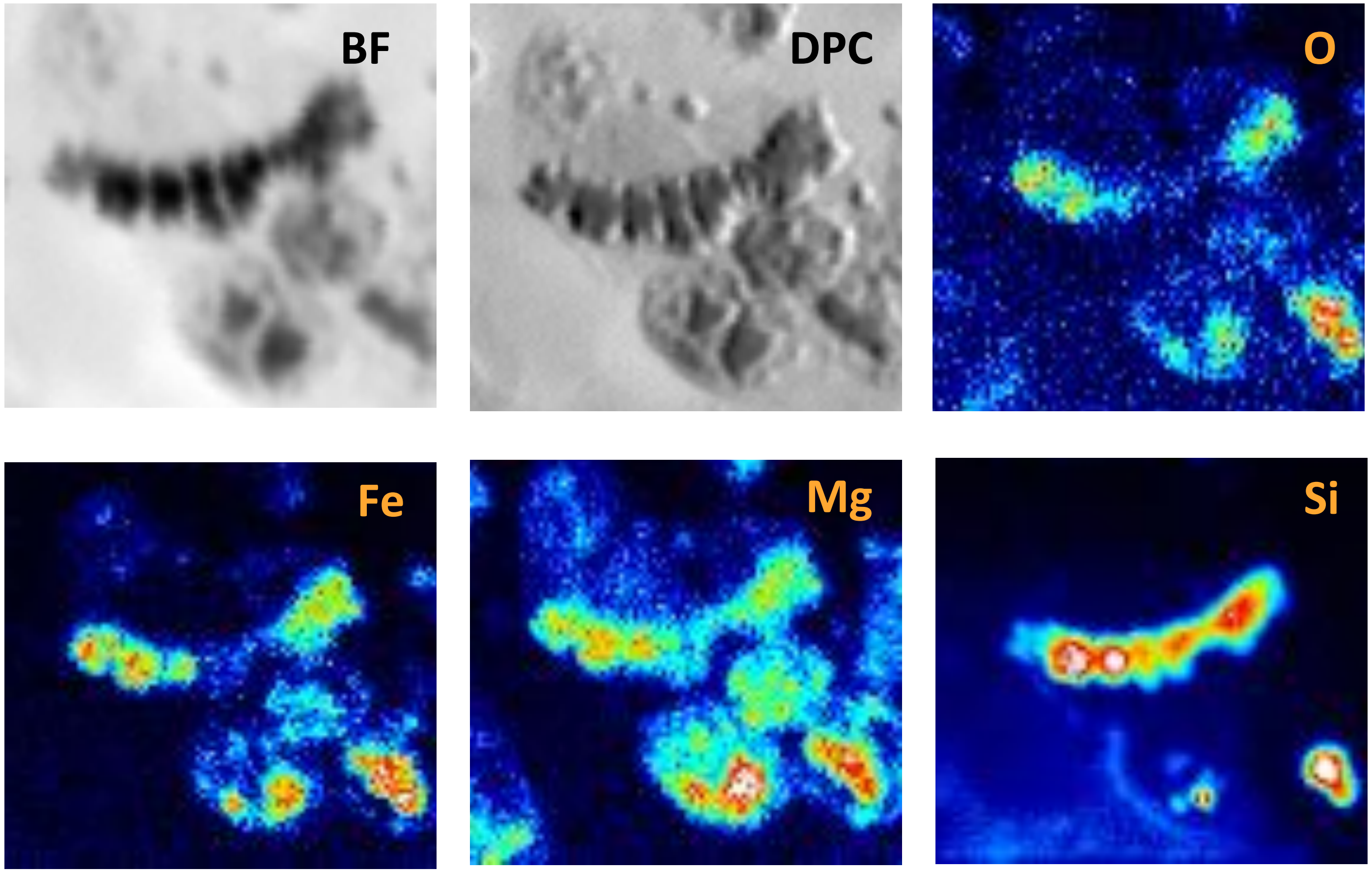

E=2019 eV, 50mm x 50 mm, 100 x 100 pixels,   15s/pixel
LEXRF

L. Pascolo, A. Gianoncelli, B. Kaulich, C. Rizzardi, M. Schneider, C. Bottin, M. Polentarutti, M. Kiskinova, A. Longoni, M. Melato, Synchrotron soft X-ray imaging and fluorescence microscopy reveal novel features of asbestos body morphology and composition in human lung tissues, Particle and Fibre Toxicology 2011, 8:7.

Biotechnology: Al in tea leaves

Charlotte Poschenrieder,
Uni Barcelona, ES
Katharina Vogel,
Uni Ljubljana, SI

Functionality and toxicity of Al in tea leaves analyzed on sub-cellular level

Cross-section of a leaf

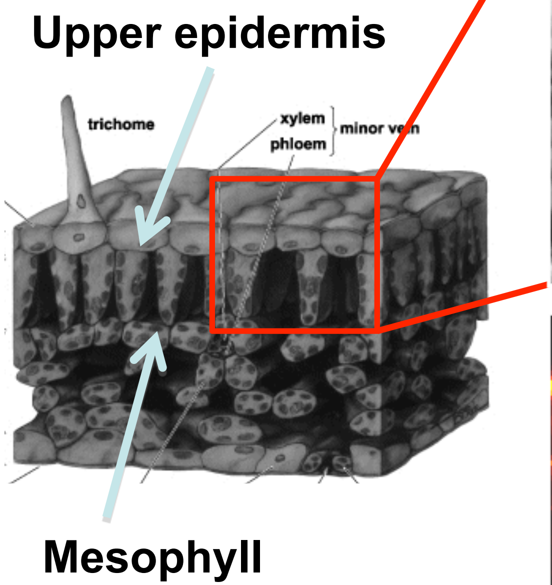

E=2.19 keV
80 x 80 μm², 80 x 80 px
12s /px

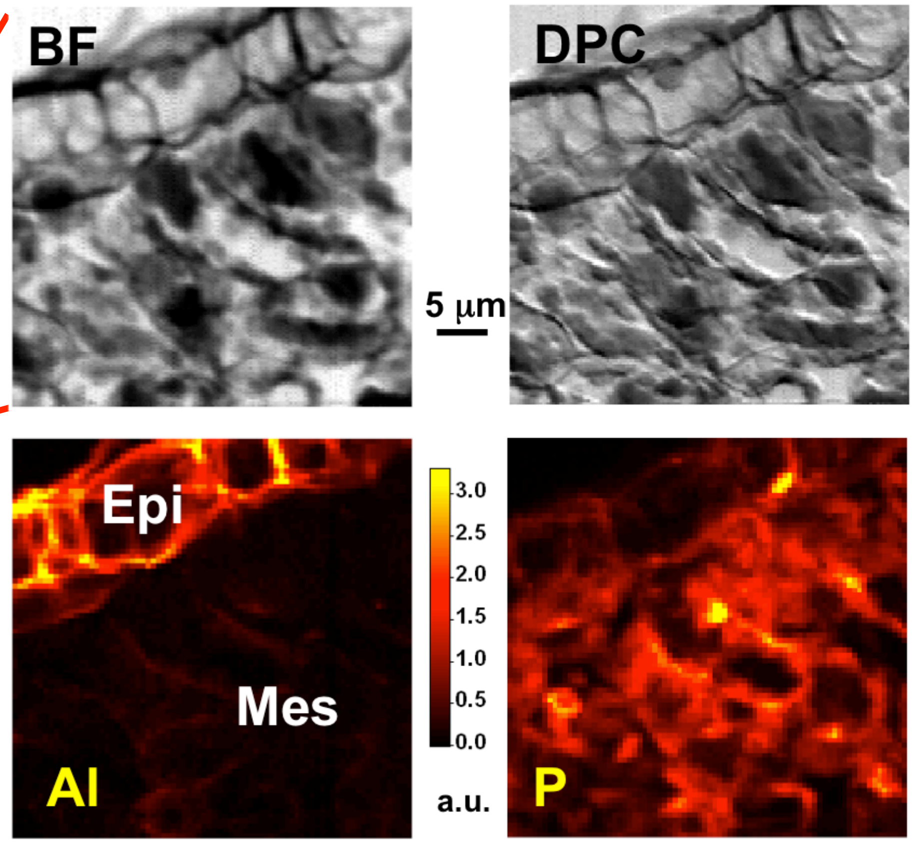

In young tea leaves the preferential accumulation of Al occurs at the end of the transpiration stream, in the epidermal cell walls

R. Tolra, K. Vogel-Mikus, R. Hajiboland, P. Kump. P. Pongrac, B. Kaulich, A. Gianoncelli, V. Babin, J. Barcelo, M. Regvar, C. Poschenrieder, *Localization of aluminium in tea (Camellia sinensis) leaves using low-energy X-ray fluorescence spectro-microscopy*, J Plant Research 124, 165-172.

Conclusions

- Synchrotron radiation facilities provide state of the art techniques
- Synchrotron radiation X-ray microscopy techniques offer high spatial resolution (through absorption and phase contrast imaging) and high chemical sensitivity (through XRF contrast)
- Different contrast techniques are available, suitable to specific applications
- Wide range of applications
- Complementariety to other techniques (laboratory, SR...)